

Received February 21, 2022, accepted March 14, 2022, date of publication March 22, 2022, date of current version April 14, 2022.

Digital Object Identifier 10.1109/ACCESS.2022.3161564

# Wearable Textile Patch Antenna: Challenges and Future Directions

M. M. HASAN MAHFUZ<sup>1</sup>, (Student Member, IEEE),  
MD RAFIQUK ISLAM<sup>1</sup>, (Senior Member, IEEE),  
CHAN-WANG PARK<sup>2</sup>, (Senior Member, IEEE), ELFATIH A. A. ELSHEIKH<sup>3</sup>, (Member, IEEE),  
F. M. SULIMAN<sup>3</sup>, (Member, IEEE), MOHAMED HADI HABAEBI<sup>1</sup>, (Senior Member, IEEE),  
NORUN ABDUL MALEK<sup>1</sup>, (Senior Member, IEEE),  
AND NAZMUS SAKIB<sup>1</sup>, (Student Member, IEEE)

<sup>1</sup>Department of Electrical and Computer Engineering, Faculty of Engineering, International Islamic University Malaysia (IIUM), Kuala Lumpur 53100, Malaysia

<sup>2</sup>Department of Electrical Engineering, University of Quebec at Rimouski, Rimouski, QC G5L 3A1, Canada

<sup>3</sup>Department of Electrical Engineering, College of Engineering, King Khalid University, Abha 62529, Saudi Arabia

Corresponding author: Md Rafiquk Islam (rafiq@iium.edu.my)

This work was supported by the Deanship of Scientific Research at King Khalid University through the Research Group Program under Grant R.G.P.1/219/42.

**ABSTRACT** Wearable antennas have grown in popularity in recent years as a result of their appealing features and prospects to actualize lightweight, compact, low-cost and adaptable wireless communications and surroundings. These antennas have to be conformal and made of lightweight materials in a low-profile arrangement when attached to various parts of the human body. Near-body operation of these antennas should be possible without degradation. When these characteristics are taken into account, the layout of wearable antennas become challenging, especially when textile substrates are investigated, high conductivity materials are used during manufacturing procedures and body binding scenarios have an impact on the design's performance. Several of these issues arise in the context of body-worn deployment, despite modest changes in magnitude between implementations. This paper examines the multiple issues and obstacles encountered in the construction of wearable antennas as well as the range of materials used, and the Specific Absorption Rate (SAR) effects employed as well as the bending scheme. An overview of the innovative features and their separate approaches to addressing the difficulties lately raised by work in this field conducted by the scientific community is provided as an appendix.

**INDEX TERMS** Wearable textile antenna, WBAN, SAR, 5G, ISM, WLAN, UWB, C-band, X/Ku-band, microwave imaging, human body, bending effect and flexibility, crumpling, wrinkling, laundering, mimics effect, CP, EBG, metamaterial, AMC, HIS.

## I. INTRODUCTION

The meaning of “wearable antenna” is the flexible and efficient system connected with the human body for wireless communication. In addition to safety, health and living standards, the design and creation of these systems is of utmost importance [1]. People are now much more interested in antenna used for body-centric communication since they see it as an increasingly popular kind of communication [2] which used in body part-based physically implemented elements for capture and data communication. In wearable technology the most dominating research issue is textiles or fabric-based antennas [3]. Since clothing is an everyday

necessity for most people it makes sense to incorporate electrical devices in their clothes and turn them into smart clothing. With the wearable antenna people can live their lives more comfortably and without difficulty [4], [5]. While individuals tend to be concerned about their personal security and the health effects of technology body worn antennas have become popular for everyday uses [6]. A smart textile has applications in a number of diverse disciplines including the sports, fashion, military, medical and healthcare sectors [7]–[9]. The criteria of most applications are light weight, low cost, nearly maintenance free and easy to install, which is why the wearable antenna fulfils these needs [10]. It is essential to have an antenna that is smaller in size and more durable to achieve the aforementioned requirements [11]. The antenna described here are appropriate for

The associate editor coordinating the review of this manuscript and approving it for publication was Debabrata Karmakar<sup>1</sup>.

everyone from the elderly to athletes and they are used to monitor various activities [12]. Textile-based antennas are especially reliant on fabric while in development. To produce a high-performance antenna system the fabric must be lightweight and pourable [13], [14]. At the time of design it was ensured that the radiator would not cause injury to the body tissue [15]. A great deal of progress has been made in the field with the extra demands.

One of the major issue in wearable antenna is the consistency of characteristics across varied environment. It addresses such aspects as temperature, humidity and the proximity of people and other garments as well as wash cycles, etc [9], [16]. There are multiple directions a user might follow therefore motion causes scattering. Wave polarization is influenced by movement of various bodily parts such as arms, legs, and eyes, causing polarization discrepancy [17]. Many researchers have a keen interest in fixing all these difficulties right now. The textile antenna design requires an investigation into electromagnetic properties of textile materials linked to permittivity and loss tangent [18]. Textiles may be classified as conductive or non-conductive or, even as both [19], [20]. The radiating element uses conductive fabric while the substrate is made from nonconductive fabric [21]. Conductive textiles such as Zelt and Flectron as well as nonconductive textiles such as silk, felt and fleece fabric are examples of this type of material [22]. There are various techniques of determining the dielectric characteristics of textiles that are included in [23]. Furthermore, microstrip patch antennas provide numerous advantages for on-body wearable electronics in addition to their directivity advantages [24]–[26]. The three most important advantages are: simplicity of design, low cost and the decrease in the amount of energy used by the skin all of which are attributed to the ground plane, which is between the radiating component and the surface and offers separation [27]. The patch antennas are limited in bandwidth and may need to be large to eliminate interference with the body [28]–[30]. This article is laid out as follows: Section has been offered a general introduction to wearable antenna designs, their capabilities and their applications. Section II introduces the reader to the various types of wearable antennas, their performance characteristics and potential uses. A textile wearable antenna was tested for its performance in terms of its size substrate and frequency range. Section III as well how different bending conditions and crumpling affect the antennas performances. Section IV detailed the SAR values and techniques for lowering them. Section V concludes the entire article by providing a summary of the main challenges and future directions of research.

## II. SUBSTRATE AND DESIGN OF ANTENNAS

A smart fabric is any cloth whose hardware gives the wearer a digital device. Smart clothes, e-textiles, smart materials and garments tracking are all examples of smart fabrics. It all started in the mid-20th century when [31], in 1977 created a conductive polymer and earned the Nobel Prize thirty-three years later. Apparel with textiles are notable for employing

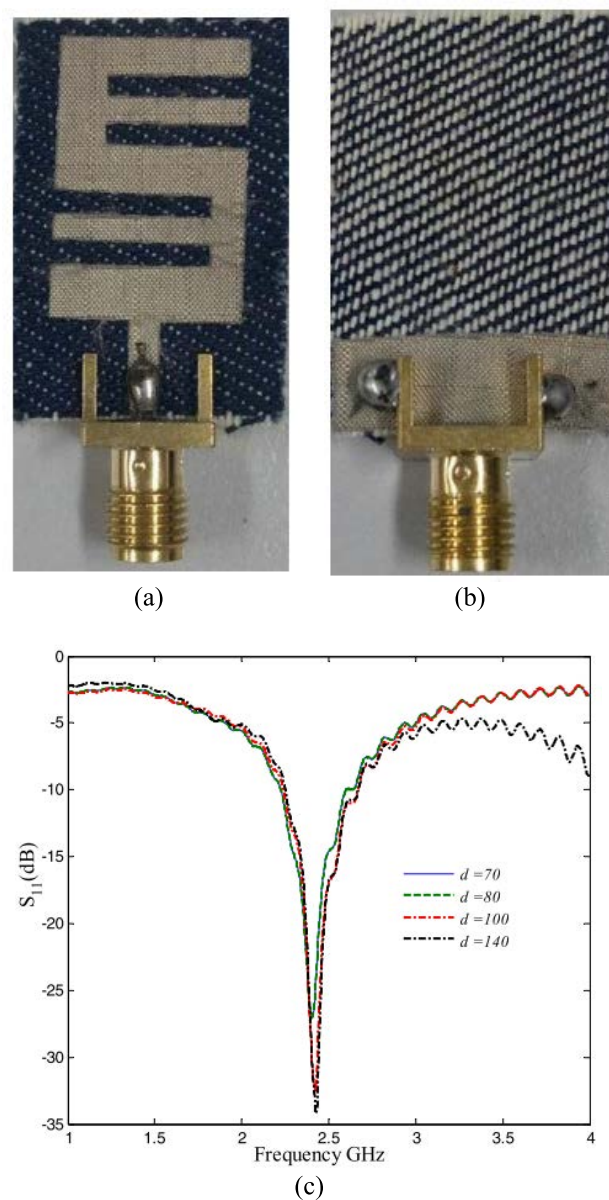


**FIGURE 1.** An E-shaped fabricated antenna (a) top view, (b) bottom view and (c) return loss [34].

antennas with which wireless properties can be discovered, identified, analyzed, controlled, etc. without causing the user discomfort [32]. Smart wearable antennas are gaining in popularity because of the recent developments in fashion technology. As a result of their vast range of potential applications which include health control, sports, navigation and military, wireless systems have received more attention in recent years [33]. Therefore, the design and demonstration of a miniaturized textile antenna (denim substrate) shows in Fig. 1 for ISM band application at 2.4 GHz are presented [34]. An E-shaped antenna is formed by placing a strip line between two rectangular slots. This basic, small and fabric-only construction is ideal for manufacturing. When compared to a normal antenna this antenna is 75%

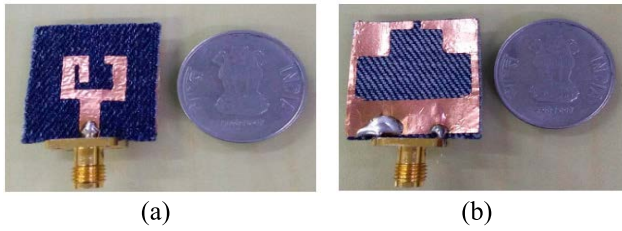


FIGURE 2. Fabricated jeans textile antenna (a) top & (b) bottom view [35].

smaller [34]. Bending the antenna reveals it can retain its overall performance, while being deformed. An improvement in size downsizing of 30 mm×20 mm×0.7 mm is demonstrated by the antenna, which has an impedance bandwidth of 15% and an efficiency of 79%, indicating that it is a suitable candidate for insertion into wearable devices. A laboratory experiment studied the effect of bending on antenna performance the results demonstrate negligible effect. A full circuit design was developed for the proposed design and the findings showed a good correspondence with the simulation results. In total, because of its low manufacturing costs, small size and acceptable radiation and, bandwidth performance, the antenna presented is an appropriate choice for ISM (2.4 GHz) application.

In the same way, it is proposed to use a textile antenna (jeans) for the WLAN, C band and X/Ku band frequencies [35]. This textile antenna is constructed on the inside of jeans denim fabric to help limit the effects of surface waves. This antenna design has a patch, which is then grounded through a diffracted ground structure illustrated in Fig. 2. Microstrip feed line technique has been used to design of the wearable textile antenna. In the three frequency bands shows in Fig. 3, the achieved impedance bandwidths are as follows: 3.4–4.3 GHz (23.37%), 4.7–8.4 GHz (56.48%) and 10.3–14.1 GHz (31.14%). The max gain has been measured at 4.1 GHz, is 4.85 dBi. The SAR value was determined in order to observe the radiation effect, and it was discovered that its maximum SAR value at 5.2 GHz and 5.5 GHz is 1.8418 W/kg and 1.919 W/kg respectively, which is less than 2 W/kg of 10 gm tissue. When comparing findings obtained from simulations and measurements, the measurement results were quite similar to simulation results. As a result, a sound explanation was established. This textile antenna is suitable for use in the circularly polarized triple band with good radiation performance, gain, and SAR values, that are within acceptable limits.

In [36], a multilayered polyester fabric with an E-shaped microstrip patch antenna was proposed for Wi-MAX application. The most difficult issues in the design of a textile antenna were ensuring that the textile substrate had an appropriate thickness, surface homogeneity, and water wettability characteristics. The polyester fabric has a high-tech, polyvinyl alcohol (PVB) coating and shows hydrophobic behavior with an angle of 91°. Uncoated polyester fabric had an RMS roughness of 341 nm. PVB-coated polyester fabric had an

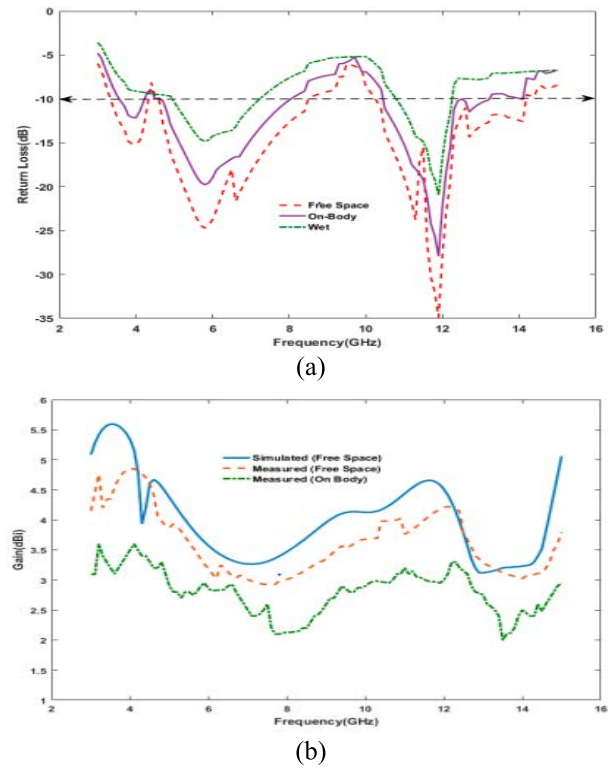


FIGURE 3. Jeans textile antenna's simulated and measured (a)  $S_{11}$  & (b) gain [35].

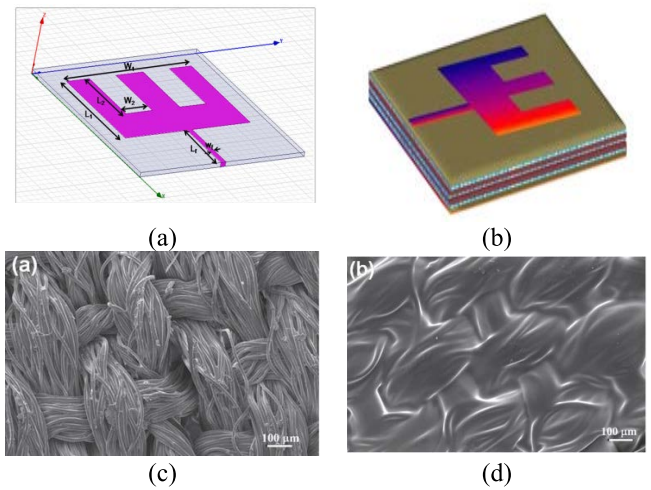
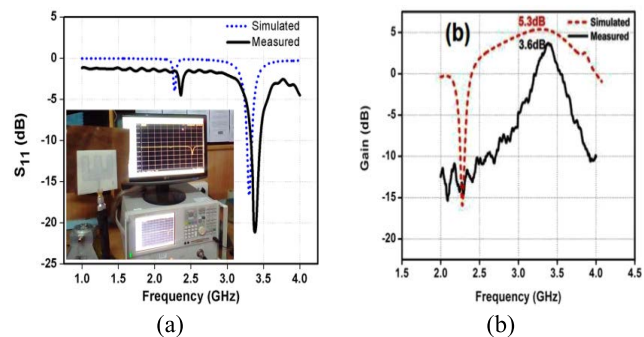


FIGURE 4. Physical layout of the E-shaped antenna (a, b) and uncoated, coated polyester fabric's cross section respectively (c, d) [36].

RMS roughness of 15 nm and the proposed antenna's layout illustrated in Fig. 4. As a result of its advantageous characteristics, such as their flexibility, light weight, and low cost, the suggested antenna can be easily integrated into clothing such as polyester jackets. In order to demonstrate the utility of the fabricated antenna's prototype, simulation and measurement results were displayed in terms of return loss and gain shown in Fig. 5. The tested antenna successfully



**FIGURE 5.** E-shaped antenna’s simulated and measured results (a)  $S_{11}$  & (b) gain [36].

operated at 3.37 GHz with a return loss of  $-21$  dB and a maximum achieved gain of 3.6 dBi. By virtue of its thin, flexible, and water-resistant design, the produced antenna may be integrated into new generation apparel like jackets, which not only sense and convey data but also provide others with useful information.

In [37], future wireless systems will benefit from the use of a revolutionary wearable textile antenna that will function at 2.45 GHz and 5.8 GHz in ISM band and the industrial, scientific wireless communication purpose. This proposed wearable antenna created a negligible impact on the human body and can be easily manufactured on jeans fabrics. Because of its exceptional operation bandwidth, compactness, and integration into clothing qualities, the proposed antenna is suitable to be used to create wearable antennas that are integrated with the human body in the near future. Fig. 6 illustrated the fabricated antenna’s prototype with tested return loss. A small textile antenna (jeans fabric) that is suitable for UWB application has been developed in [38]. This proposed antenna achieved (2.96–11.6) GHz bandwidth for UWB application and maximum gain 5.47 dBi at 7.3 GHz. In order to complete the mathematical analysis, the cavity model of antenna was used in conjunction with circuit theory, which proved to be a proposed design. In order to provide a partial ground plane, various slots and notches were deleted from the radiating patch which is shown in Fig. 7, and the impedance-matching performance of the system was demonstrated by current distribution. A study was carried out to determine the antenna’s SAR value in order to demonstrate the radiation’s effect on the human body. It was found that the antenna’s SAR value is 1.6018 W/Kg, which is less than 2 W/Kg of 10 gm tissue. This point shows what results the antenna produced, making it clear that it is different from other antennas. Based on these findings, it has been believed this clothing-embedded medical device may be used in telemedicine and mobile health systems. The simulated and measured return loss and gain illustrated in Fig. 8.

WBAN applications have a wide range of potential uses, including the remote monitoring of patient health and the transmission of data wirelessly. Wearable antennas make patients more comfortable while monitoring, as well as the

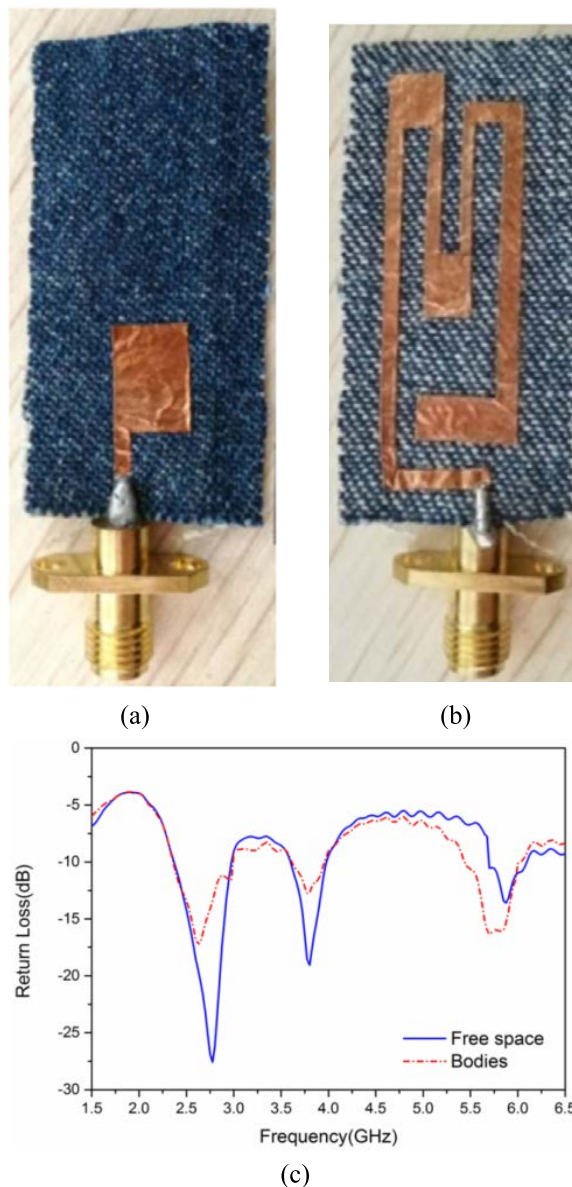


**FIGURE 6.** Novel wearable textile antenna wearable textile antenna (a) top, (b) bottom view and (c)  $S_{11}$  [37].

continuation of their health care. As a result, they must be convenient, flexible, and capable of operating without causing severe degradation near the human body. To provide a large bandwidth while maintaining SAR within acceptable limits for both 1 gm and 10 gm tissue standard, a full-ground UWB antenna is developed and used in this research paper [39]. Denim textile substrate has been used to simulated and fabricated purpose Fig. 9 illustrated the fabricated proposed antenna and return loss. Apart from that, it is anticipated that the proposed antenna has a large bandwidth from 7 to 28 GHz, maximum directional gain of 10.5 dBi, and a maximum radiation efficiency of 96%. A SIW transition and GCPW were used to feed the antenna. Following the investigation of the antenna’s performance in free space, its

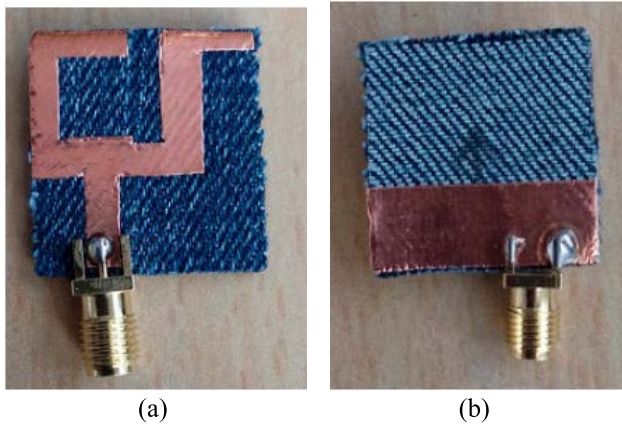


FIGURE 7. Jeans textile UWB fabricated antenna [38]. (a) Top View (b) Bottom View.

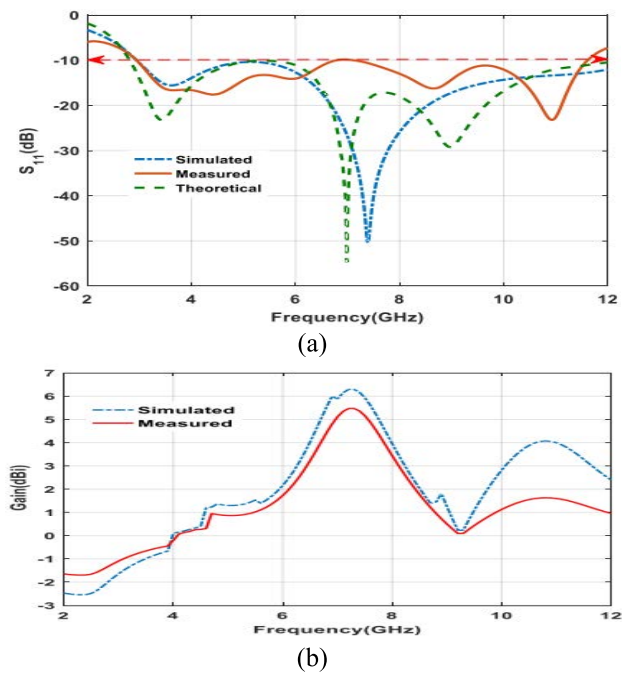


FIGURE 8. Simulated and measured (a)  $S_{11}$  & (b) gain [38].

radiation properties are investigated in a new medium, the breast tumor in order to detect in various scenarios, including central tumors with and without skin, and numerous tumors (two and three) within the breast. Because of its strong performance on a soft medium such as a breast, the reconstructed images demonstrated that the antenna could be an acceptable option for use as part of a wearable WBAN system for breast cancer surveillance and imaging.

In [40], proposed the construction of a dual-band, miniature-structured wearable antenna. This antenna is created for the ISM band, which includes frequencies between 2.45 GHz and 5.8 GHz. Choose denim as the material for the base, and copper tape as the radiating element. Simulated and measured results showed that the antenna has

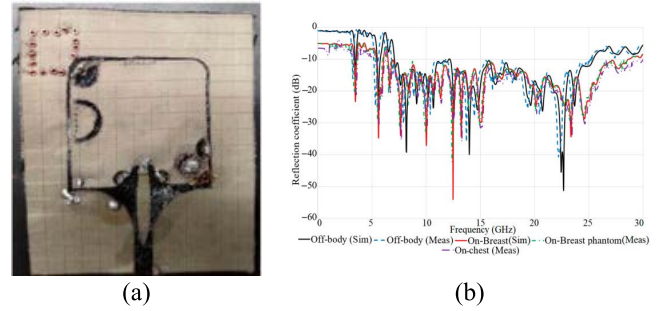


FIGURE 9. Denim textile substrate fabricated antenna (a) and return loss (b) [39].

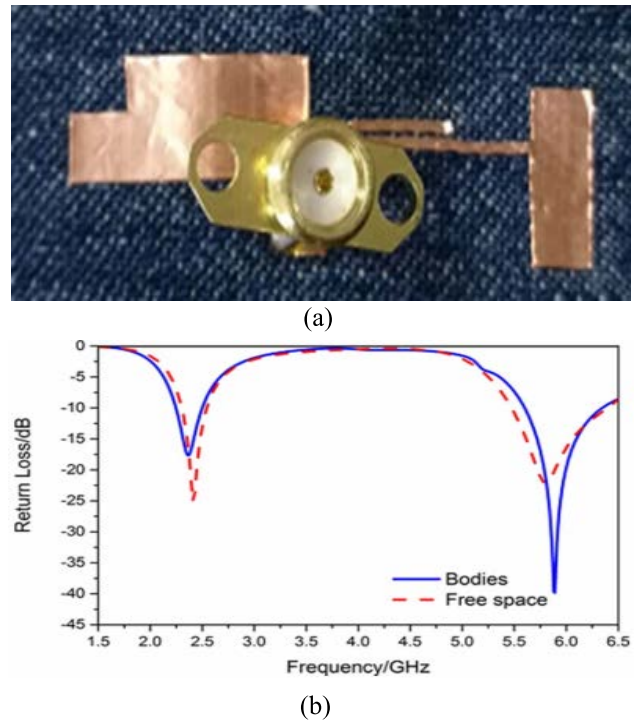


FIGURE 10. Miniature-structured wearable antenna (a) & return loss (b) [40].

excellent performance on ISM band. The proposed fabricated antenna and its measured return loss illustrated in Fig. 10. The measured results discovered that, when the antenna was positioned near the human body, the antenna’s performance was only minimally influenced. To make matters even better, the antenna has the excellent properties to be suitable for both portable and wearable electronics.

In [41], illustrates the impacts of curvature on the operation of a rectangular textile patch antenna, which is used in industries, research, and medicine at 2.4 GHz frequency (ISM). The antenna’s base was denim fabric, while the conducting layers were copper and nickel-plated polyester fabric and Fig. 11 illustrated the fabricated antenna. To study the influence that textile antenna has on WBAN performance, researchers evaluated the bending of the WBAN signal at three general locations: the chest, arm, and wrist. This study reveals that the curvature of the bending plays a critical role in

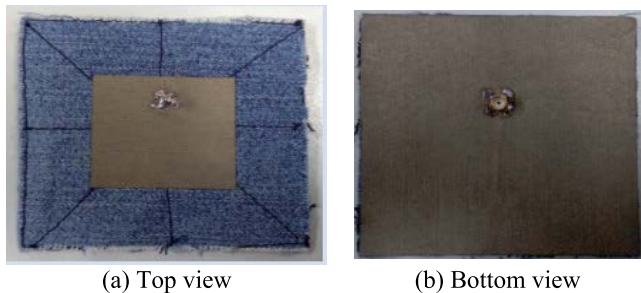


FIGURE 11. Fabricated rectangular textile wearable antenna [41].

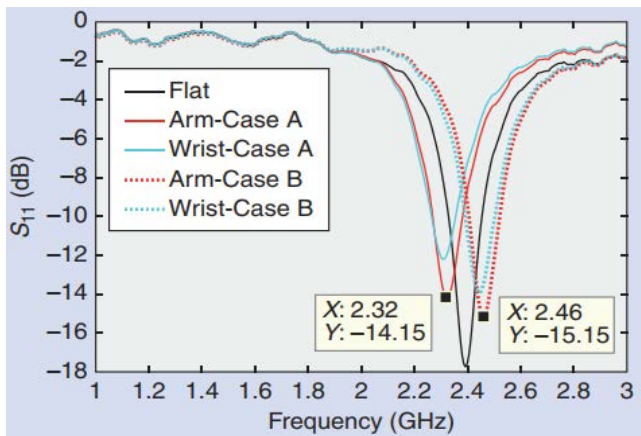


FIGURE 12. Rectangular textile patch antenna's measured  $S_{11}$  [41].

the magnitude of gain and radiation pattern. When compared to a flat antenna enclosure, the wrist comparable curvature reduces the overall gain by around 2 to 4 dBi. All cases measured show that bandwidth stays nearly the same and Fig. 12 shows the measured return loss.

An antenna with adjustable (reconfigurable) microstrip patch antenna has been described in detail in [42]. At the ground, this antenna is comprised of a rectangular patch with truncated edges, which is integrated with a slot structure at the bottom shows in Fig. 13. The ground plane has three BAR PIN diodes switches installed on it. This antenna is able to function at different frequencies to the ability to adjust the condition of the switches. Frequencies has been controlled by using diodes from (1.41–3) GHz and the measured return loss illustrated in Fig. 14. In addition, the antenna has found an AR of less than 3 dB with GPS operating frequencies from T2 to T7 with different configurations. It is likely to be beneficial to antenna use in situations where there is a possibility of wireless device end front-end connectivity.

A compact dual-band textile printed slot antenna with a partial ground plane is shown in this research [43]. To create the designed antenna's substrate, the fabric from jeans substrate is utilized. In addition, the patch and ground plane are produced using copper tape and physical prototype illustrated in Fig. 15. Measured impedance bandwidth: From 3.01 GHz to 5.30 GHz, 8.12 GHz to 12.35 GHz shown in Fig. 16. According to the results of the reflection coefficient,

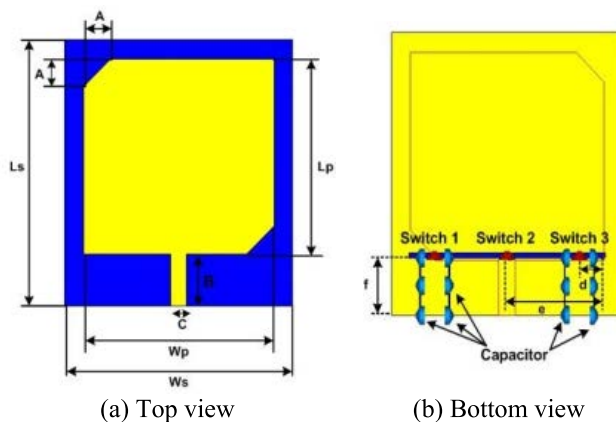


FIGURE 13. Prototypes of adjustable (reconfigurable) microstrip antenna [42].

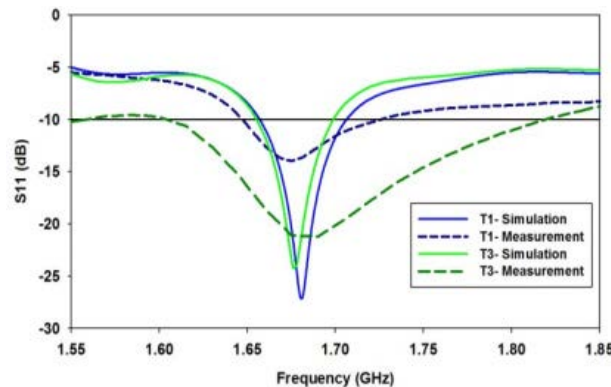


FIGURE 14. Adjustable microstrip patch antenna's measured return loss [42].

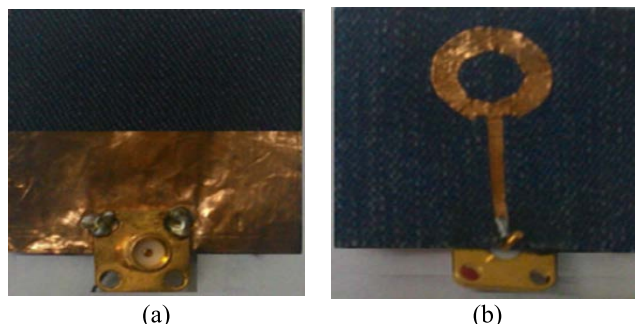


FIGURE 15. Fabricated printed slot antenna (a) front & (b) back view [43].

jeans fabric has good potential as a textile wearable. The results demonstrated that the antenna design proposed in this study had high gain, high efficiency, and continuous radiation

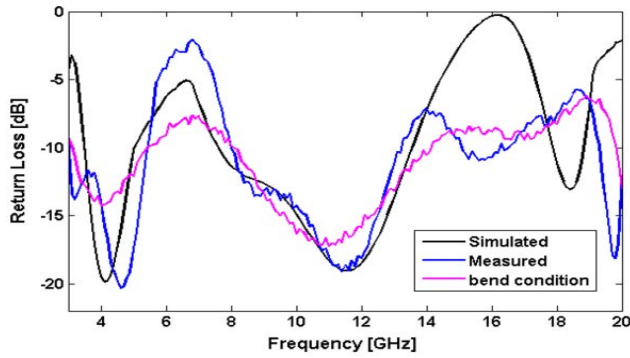


FIGURE 16. Printed slot antenna’s simulated and measured  $S_{11}$  [43].

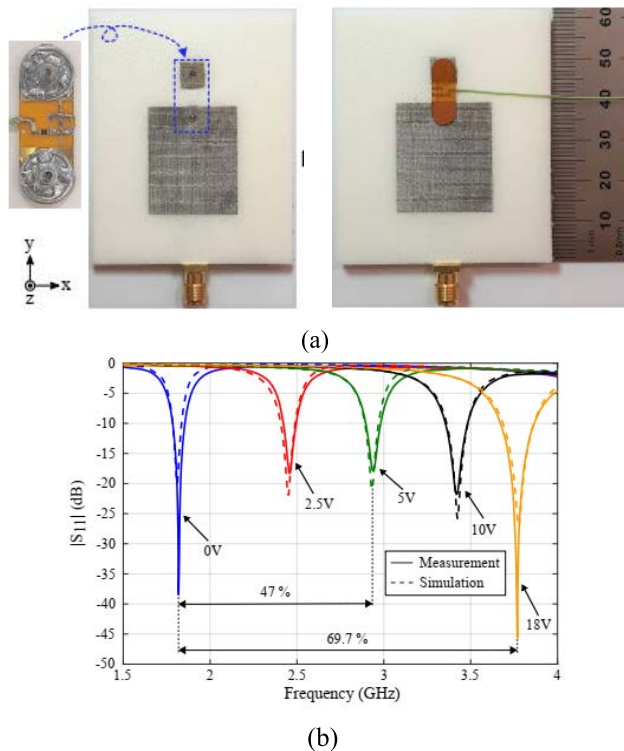
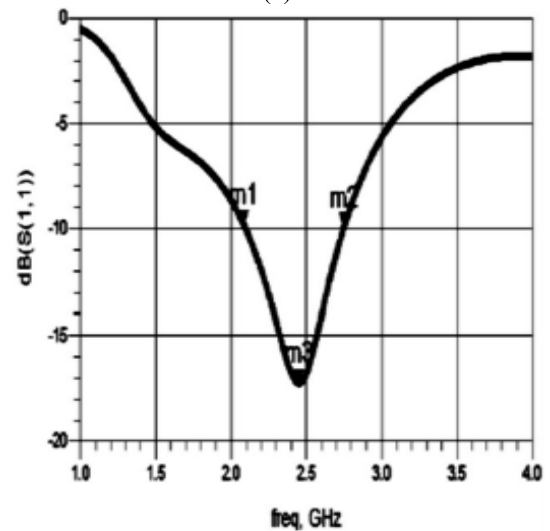


FIGURE 17. Configurable wearable textile antenna’s prototype (a) & return loss (b) [44].

patterns over its whole frequency range. This research [44] develops an antenna that can be configured to adjust its frequency range by both wearable textile. A coplanar reconfiguration module is added to a planar inverted-F antenna (PIFA) built in textile technology to allow for frequency agility. In order to reconfigure the device, a small flexible printed circuit board (PCB) is used, which contains a tuning circuitry as well as commercial Snap-On buttons that function as electronic-to-textile interfaces. In this module, a varactor diode is utilized to study and optimize the frequency re-configurability of the PIFA, then a smooth transition from a quarter-wave to a half-wave resonant mode is utilized to maximize tuning range shows in Fig. 17. The fundamental objective of recent antenna development is to achieve smaller, and simpler designs [45]. Smaller, less bulky antenna is incredibly useful in medical fields. This work



(a)



(b)

FIGURE 18. Snapshot of fabricated jeans textile antenna’s top, bottom view (a) & measured return loss (b) [45].

presents a monopole antenna (Fig. 18a) that uses textile substrate (jeans) to construct a basic structure that is lightweight and operates in 2.45 GHz ISM band. The denim jeans substrate, due to its inadequate characterization of dielectric characteristics, results in an undesirable performance reduction. As well, there is a possibility of errors in the fabrication process. When the simulated results and the observed results match, then the return loss (Fig. 18b) is considered to be valid. Simulated and measured  $S_{11}$  result of the ISM band operation band are completely covered. Those articles [46], [47] describes a new type of flexible wideband dipole antenna for upcoming medical and human body applications, using inkjet printing.

In [11] research work, proposed an alternative design for a UWB textile antenna that can be used in wearable microwave medical imaging devices. The antenna has a monopole structure that includes two triangles and a few parallel slots to obtain an optimal UWB with smaller size. The antenna is constructed, from polyester textiles and conductive copper taffeta, which are readily accessible on the market and proposed antenna illustrated in Fig. 19a. Wearable applications

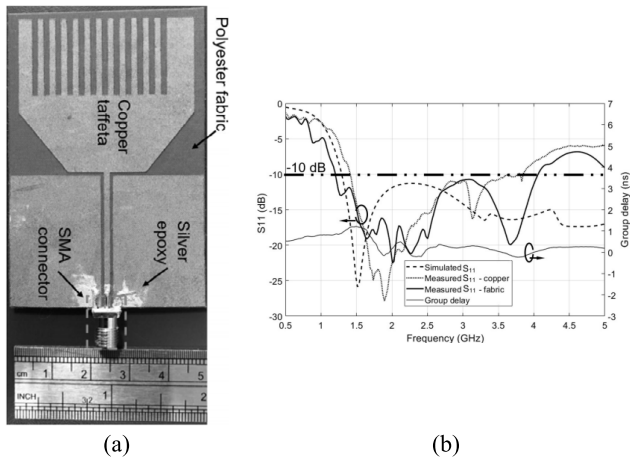


FIGURE 19. Fabricated UWB textile antenna's prototype (a) & return loss (b) [11].

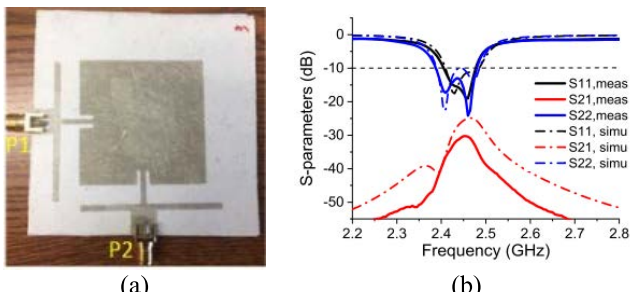


FIGURE 20. Fabricated dual port antenna textile antenna's porotype (a) & measured return loss (b) [48].

demand flexible components which can flex with the curvature of the human body. Additionally, the antenna can maintain its performance even if it is bent or while it is working in close proximity to tissue-imitating phantoms. The gain of 2.9 dBi, the antenna prototype was able to reach a bandwidth 109% of (1.198–4.055) GHz that is shows in Fig 19b. Antenna is used to observe the recovery phase of a bone fracture that is imitated by a size-varying blood strip that is used to emulate a phantom body with a fracture.

The goal of dual port antenna [48], is to allow 2.45 GHz ISM-band full-duplex wearable devices to have a smaller, lower profile design while satisfied ISM bandwidth. This textile antenna has a superior structural flexibility and excellent production precision due to the use of an innovative screen-printing process. In order to increase the bandwidth at the two input ports, an innovative solution is provided for the first time, in which two more strips are inserted into the antenna design. To produce the second-order resonant qualities with increased bandwidth, more straplines are positioned perpendicular to the feed lines illustrated in Fig. 20a. To ensure the connection between structure remain strong, structural deformation of the antenna is assessed by bending it at 0° and 45°. Experimental verification of the design concept was

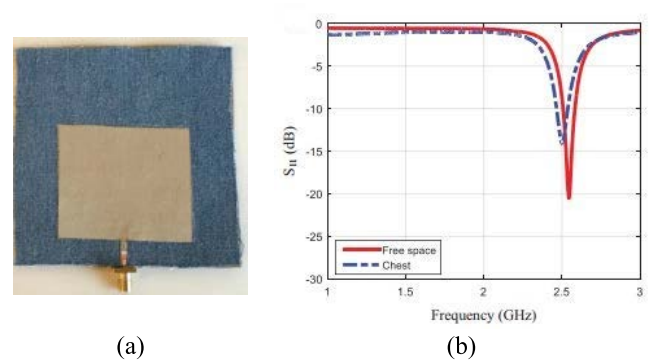


FIGURE 21. Picture of fabricated embedded circuits textile antenna (a) & return loss results (b) [49].

accomplished through measurement result (Fig. 20b) that were reasonably consistent with simulations.

Because wearable electronics are becoming more commonplace, the urge to embed circuits and antennas inside garments is proposed [49]. Electronic textiles (e-textile) could be used to achieve this integration. Changing environmental and wear circumstances can have an impact on the conductive data communication performance of an e-textile, including the resistivity of the textile's surface and the radiation properties of its antenna. To investigate the resistance of e-textiles to pilling, wrinkling, abrasion, and laundering, this research was conducted. For RF performance in this study, a microstrip patch antenna (Fig. 21a) was constructed for a wearable e-textiles, and the results (Fig. 21b) were collected under identical environmental and wear circumstances. This manuscript presents a list of limitations of the examined e-textile performance, as well as suggestions on how to enhance e-textile manufacturing for increased sustainability through wear and environmental impacts.

For wearable applications, the authors have presented [50] an unique four-layered low-profile textile antenna (Fig. 22a) that operates in ISM band (Fig. 22b). The suggested antenna was entirely textile-based, with a cotton substrate and a Zari embroidery pattern for its conducting components. The antenna also demonstrates outstanding performance and is below the IEC criterion for 1 gm and 10 gm tissue absorption. Furthermore, real-time deployment using a Particle Photon was employed to keep a constant check on the heart rate and upload the data to the Particle app via the cloud. Under bent, crumpled, moisture absorbed, and on-body conditions, the fabricated antenna was tested, along with received signal strength indicators (RSSI) and signal-to-noise ratio (SNR) readings that were made for network connected devices and round-trip times that the device required to respond to the Constrained Application Protocol (CoAP) message sent by the Particle Cloud. On examination, it was discovered that the antenna's performance remained unaltered by the deformations, making it the ideal choice for body-worn applications.

A two-band circularly polarized textile antenna is detailed in this presentation [51]. The antenna (Fig. 23a) comprises



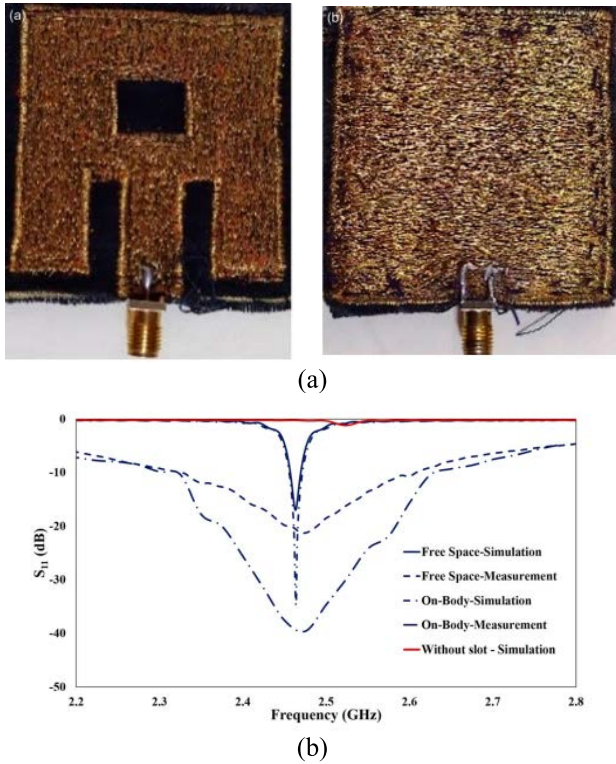


FIGURE 22. Fabricated prototype of four layer antenna (a) & measured return loss (b) [50].

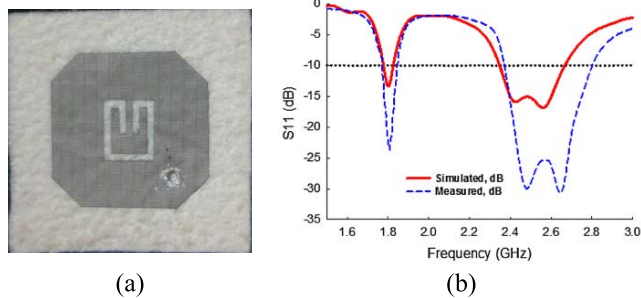


FIGURE 23. Fabricated circularly polarized antenna (a) & combination of simulated and measured return loss (b) [51].

of a slotted split ring textile patch with a full ground plane. The suggested square radiator is modified with the use of a slotted split-ring in order to accommodate dual-band resonance. In addition to covering the complete 1.8 and 2.6 GHz bands for Fourth-Generation LTE, the antenna can also cover the 2.45-GHz spectrum for WLAN applications, which is a significant improvement over previous model. The results of simulations and measurements (Fig. 23b) were in good agreement, indicating that the technology would be suitable for use in the 4G and WLAN bands.

A new dual-band, dual-polarized antenna [52], is described that operates at 2.45 GHz for both the industrial scientific, and medical bands and at 5.8 GHz for the vertical band. The design of the proposed antenna (Fig. 24a) is made up

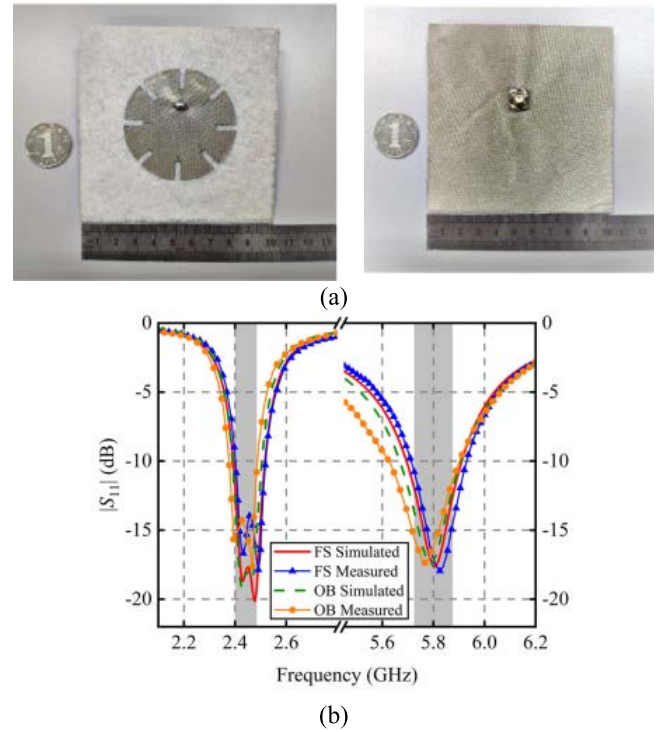


FIGURE 24. Manufactured dual-polarized textile antenna's prototype (a), combination of simulated and measured  $S_{11}$  (b) [52].

of a circular patch with eight slots, and it's made from textile material. Free-space and in-body investigations are performed to analyze the antenna's performance. The different bending antenna's radius will be used to study (Fig. 24b) the antenna's influence on the performance. Additionally, both bands are below the IEEE C95.3, 1.6 W/kg requirement.

A WBAN antenna [53], proposes a symmetric multilayered embroidered wearable textile antenna as shown in Fig. 25a. The suggested antenna was developed for use in industry, science, and medicine, and operate at a frequency of 2.45 GHz. It was constructed of Zari and cotton cloth. The introduction of a slot at both ends of the line has helped to increase the return loss and overall efficiency. The antenna is constructed from four layers, each of which is made by normal stitching and then stitched together to make the final structure. To determine the antenna's properties in bent, crumpled, and wet situations, its measurements are performed on the produced antenna. The outcomes of the test, including gains, bandwidth, and radiation pattern results, were shown to verify the structure's uses. Fig. 25b illustrated the combination of simulated and measured results. It also worked as a wearable system when the antenna was installed on the Arduino Uno development board.

Due to the prominence of wireless communications, the wearable devices are playing a significant part in this communication network [54]. Using the screen-printing technology, a slotted full textile microstrip antenna (Fig. 26a) was designed and produced to achieve miniaturization and

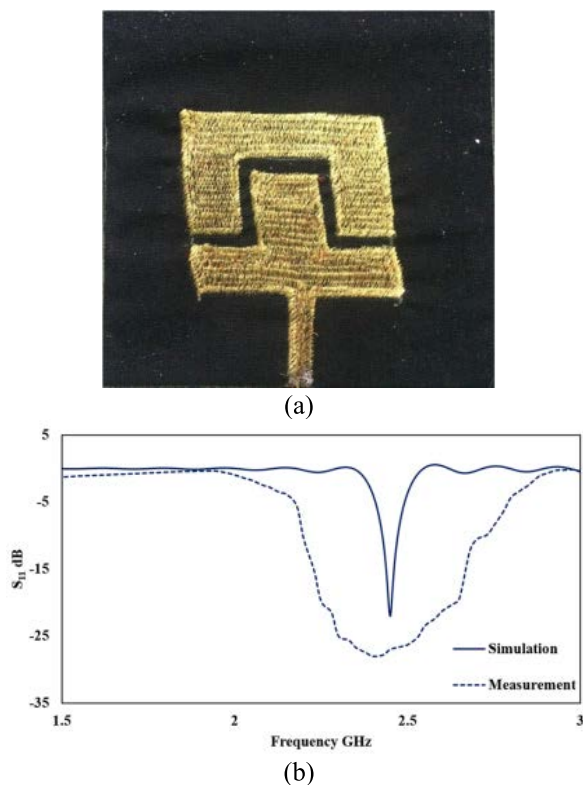


FIGURE 25. Fabricated symmetric multilayered embroidered wearable antenna's prototype (a) & reflection coefficient characteristics of the fabricated antenna (b) [53].

electromagnetic dependability. Antenna fabricated measured  $S_{11}$  and 2-D polar pattern were tested, and the results (Fig. 26b) were compared to those obtained through simulation. In addition, the study of the adhesive bonding between the silver paste coating and the textile substrate also employed the use of adhesive tape and was confirmed with the use of a microscope. To build the in-body antenna system, the researchers designed, optimized, and produced an artificial magnetic conductor (AMC). The test findings showed that the presence of the AMC helped reduce body coupling and backward radiation in the antenna.

A unique, flexible, wideband ink-printed dipole array antenna was recently introduced for use in upcoming medical electronics applications [55]. It transmits between 23 to 30 GHz, with frequencies of 24.5 and 28 GHz for 5G technology. This antenna design (Fig. 27 a, b), which can be quickly fabricated using screen printing, is a simple, layered screen-printing-based design. The highest peak gain of 4.2 dBi and 26.4% bandwidth were observed with both simulation and measurement result. Fig. 27c illustrated the combination  $S_{11}$  of copper laser-cut and silver-ink print antennas. Further research, is being carried out to determine the implications of an imprecise fabrication technique on the performance of the antenna.

The study by [56], focus on the reduce back radiation due to wearable antenna. The main lobe has used for long

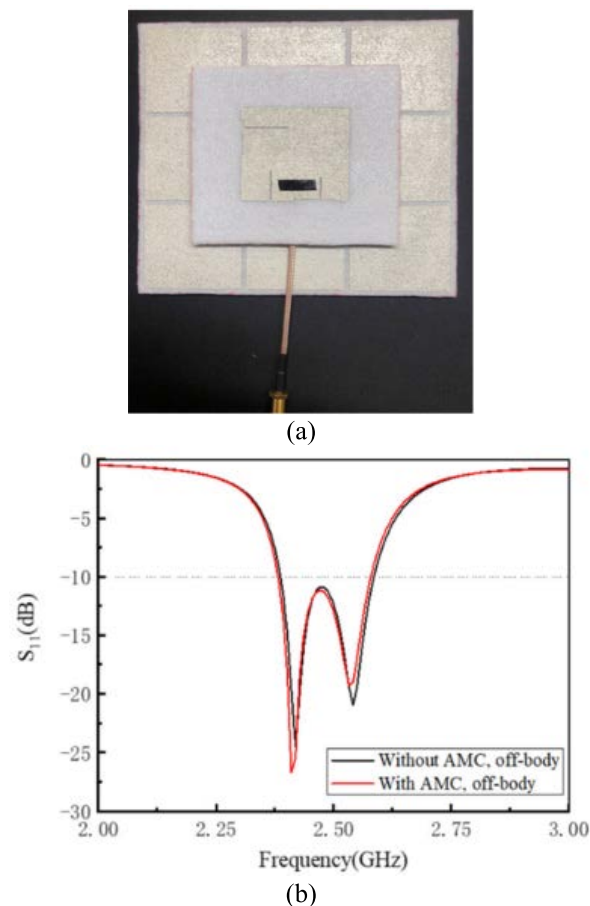


FIGURE 26. Textile slotted AMC structure antenna (a) & measured return loss (b) [54].

distance wireless communication by which radiation power of the wearable antenna must be increase for wireless communication. It is very necessary to keep the SAR values under human safety. This antenna operates at 2.45 GHz (ISM band) for medical application. Dimension of the proposed antenna  $72 \times 78 \text{ mm}^2$ , with a rectangular shape radiating patch and the SAR values shows this antenna is perfect on human body. The study also introduces different types of substrate. Fig. 28 illustrated the proposed antenna physical dimension, return loss and 2-D radiation pattern. The overall results obtained by the analysis detailed in Section II, as detailed in Table 1, were summarized.

The section substrate of antennas has presented 25 antennas and summarized Table 1. Antenna impedance bandwidth is improved by lowering surface wave losses due to, textiles which are typically with low dielectric constants. Textiles are used for portable antennas because of their high performance and adaptability. Because it raises the spatial waves, the antenna impedance spectrum becomes more favorable, allowing antennas to grow at a fair rate and with high gain. Dielectric thickness can often be employed to enhance the ibandwidth of a planar antenna, even though this approach can't maximize the antenna's overall performance. Therefore, the thickness of the dielectric material is a trade-off

**TABLE 1.** A summary of various substrates and designs used by textile wearable antennas.

Source	Size (mm <sup>2</sup> )	Frequency (GHz)	h (mm)	Substrate	Antenna Design	$\epsilon_r$	Gain (dBi)	Applications
[5]	60×60	2.45, 5.8	1	Flexible denim	Elliptical slot and C-shaped slot	1.75	2.83	ISM band
[11]	70×50	1.198–4.055	0.5	Plain-woven polyester fabric	Two triangles and parallel slots	2.193	2.9	UWB
[30]	18×19	3.09–3.94, 4.23–5.65	1	Jeans	C-shape etching slot	1.7	8.65	Wi-MAX, 5G lower band
[34]	30×20	2.4	0.7	Denim	Inverted E-shaped antenna	1.7	---	ISM band
[35]	25×25	3.4–4.3, 4.7–8.4, 10.3–14.1	1	Jeans	Tuning fork shape antenna	1.7	4.85	WLAN, C-band, X/Ku- band
[36]	50×50	3.37	1.092	Polyester fabric	E-shaped patch antenna	1.4	3.6	Wi-MAX
[37]	42×13	2.45, 5.8	1	Jeans	---	1.54	---	ISM band, 5.8 GHz
[38]	25×25	2.96–11.6	1	Jeans	Cutting notch and slot patch antenna	1.7	5.47	UWB
[39]	60×50	7–28	0.7	Denim	Ground coplanar waveguide antenna	1.4	10.5	WBAN, UWB
[41]	101×96	2.4	1	Denim	---	1.6	4	ISM band
[42]	113×99	1.41–3	1.7	Felt fabric	Rectangular patch antenna with PIN diodes	1.22	3.28	Reconfigurable frequency
[43]	40×40	3.01–5.30, 8.12–12.35	1	Jeans	Ring shaped patch antenna	1.67	5.7	Wi-MAX, WLAN, X-band
[44]	60×26	1.82–3.79	1.6	PF-4 foam	Planar inverted-F antenna	1.06	---	Reconfigurable
[45]	64.1×50	2.45	2	Jeans	---	1.57	---	ISM band
[48]	53.6×25.5	2.45	2	Planer textile	Dual port antenna	1.7	7.5	ISM band
[49]	90×90	2.45	0.56	100% cotton	Rectangular patch antenna	1.7	2	ISM band
[50]	51×45	2.45	0.785	Cotton	Rectangular patch with inset feed	1.51	---	ISM band
[51]	70×70	1.76–1.83, 2.36–2.76	3	Felt	Slotted split ring patch antenna	1.44	3.2	LTE, WLAN
[52]	100×100	2.45, 5.8	2	Felt	Circular patch antenna	1.2	---	ISM band, WBAN
[53]	58×63	2.45	2	Woven cotton	Reversed U & T shaped slot patch antenna	1.51	---	ISM band
[54]	70×70	2.45	3	Polyester felt	T-shape slot inside rectangular patch	1.4	---	ISM band
[55]	25×12.7	23–30	0.35	Polyester fabric	Dipole array antenna	2.2	4.2	5G
[56]	72×78	2.45	2	Denim fabric	Three slots and two stubs patch antenna	1.6	6.8	ISM band
[57]	50×80	2.4–2.484, 2.45, 3.3–3.9, 6.57–6.8	0.56	Jeans	Rectangular Horn-shape	1.6	4.74, 3.71	ISM band, Wi-Fi, Wi-MAX, C-band
[58]	60×80	2.4	1.6	Felt	Novel dual-port fully-textile antenna	1.2	6.3	ISM band

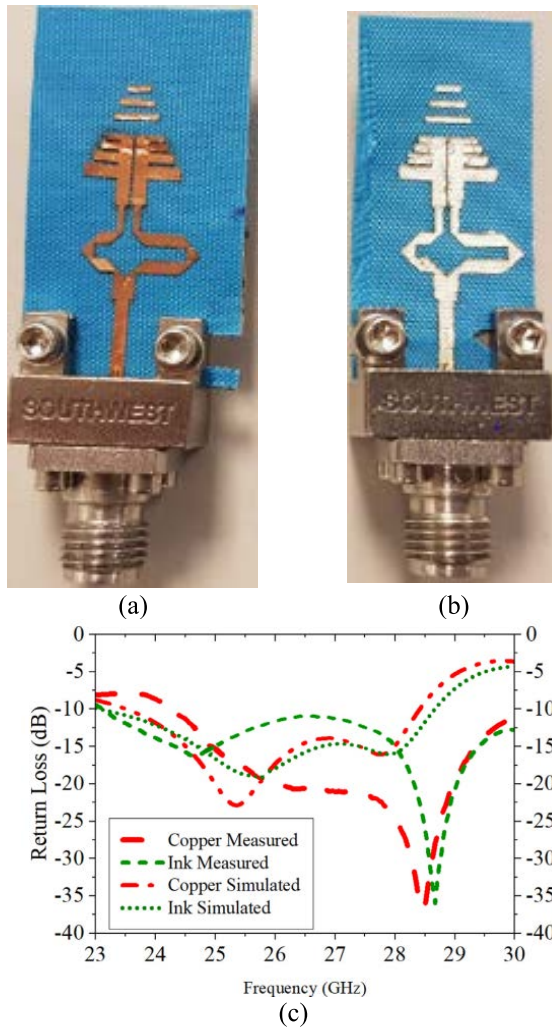


FIGURE 27. Fabricated wideband ink-printed dipole array antenna (a) copper laser-cut, (b) silver-ink printed & (c) return loss [55].

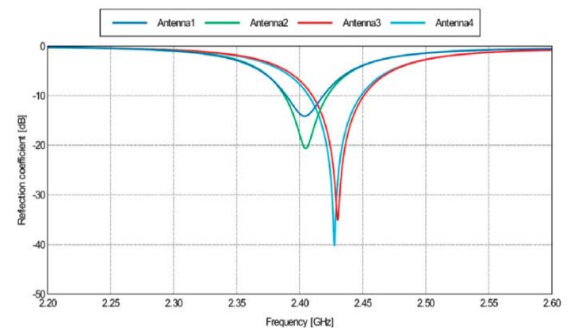
between the antenna’s gain and bandwidth. The antenna’s structural size is frequently affected by the substrate thickness. When designing an integrated wearable antennas, the trade-off between efficiency, size and difficulty in developing different (ISM band, Wi-MAX, 5G lower band, WLAN, X/K-band, Bluetooth etc.) applications must be carefully considered. This section demonstrates that, Polyester fabric, Jeans and Denim fabric has excellent impact on antenna design. In addition, those substrates are available on the market as well as cost efficient. Moreover, from this study jeans and denim substrate with C-shape etching slot on the radiating patch and ground coplanar waveguide antenna have excellent performance on bandwidth, gain as well as compact in size.

### III. BENDING EFFECTS IN TEXTILE ANTENNAS

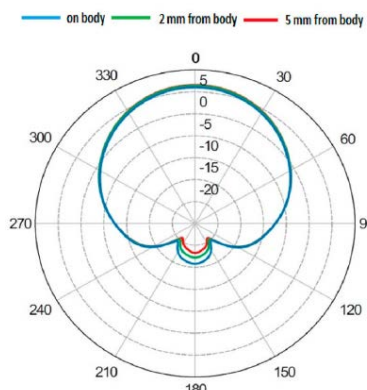
Clothing, as has been revolutionized with the creation of wearable intelligent textile systems, which features like vital sign and environmental parameter monitoring [41], [59]. Textile-based patch antennas are ideal for use in systems



(a)



(b)



(c)

FIGURE 28. Fabricated of ISM band antenna, (a) return loss (b) and radiation pattern (c) [56].

that are paired with a base station, enabling a short-range wireless communication [60], [61]. To provide ample bandwidth wireless communications, the textile patch antenna was devised [35], [38], [62]–[64]. A low-loss, lightweight, and flexible antenna was manufactured by first selecting the antenna’s design and then using only lightweight and flexible textile materials [65]–[67]. The prototype can reliably transmit information due to its high-performance communications bandwidth and gain. If it is embedded into clothing however, antenna performance can be altered by the body and bending [68]–[70].

The performance of wearable antennas must be consistent with respect to different deformations. This feature explores

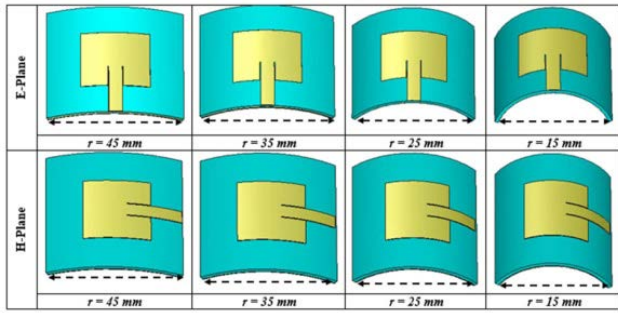
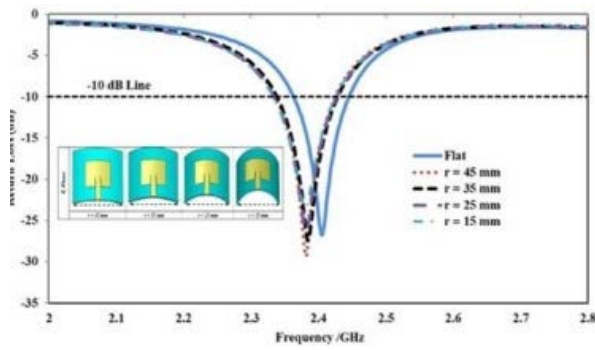
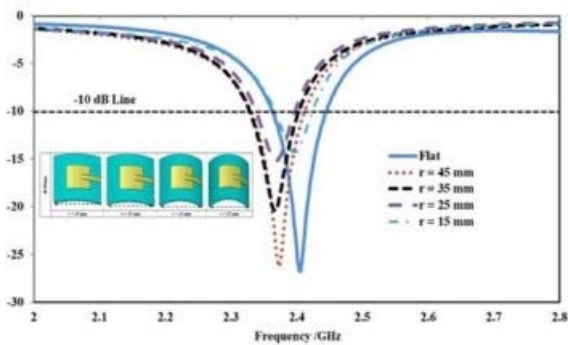


FIGURE 29. Effects of bending for various radii in E & H-plane [71].



(a)



(b)

FIGURE 30. Effect bending with different radii on  $S_{11}$  (a) E-plane & (b) H-plane [71].

the antennas bendability as their major plane radii vary and the simulated return loss is included. A research work presents the bending effect on different radii such as 0 (flat condition), 15, 25 and 35 mm is presented (Fig. 29) with E and H-iplanes [71]. The suggested antenna demonstrates a better impedance match with a return loss of less than  $-10$  dB, regardless of the E-plane (Fig. 30a) bending radius. This antenna offers improved impedance matching with a return loss of less than  $-10$  dB when bent across a 45 mm radius in the H-plane (Fig. 30b), compared to other circumstances ( $r = 35, 25,$  and  $15$  mm). The resonance frequency of the antenna is displaced a bit to the left (in comparison to the flat version), which occurs for both E and H-plane bending

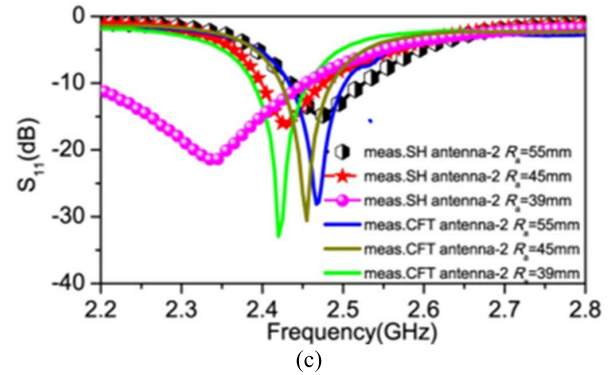


FIGURE 31. Flexible textile antenna's fabricated layout (a, b) and  $S_{11}$  of different bending radii (c) [70].

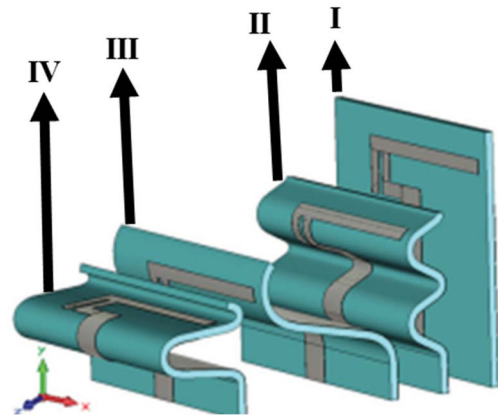


FIGURE 32. Layout of antenna in crumpling condition with crumpling depth of case I (0 mm), II (5 mm), III (24 mm), IV (25 mm) [72].

for radii are 45, 35, 25, and 15 mm. Despite this, the bent antenna's fractional bandwidth remains the same under all conditions.

In article [70], shows the bending effect on basis of 39, 45 and 55 mm radius. When the antenna is attached to a human arm, the resonant frequency changes to the right, which is outside of the required frequency band. The suggested antenna shows in Fig. 31 (a, b). Fig. 31c illustrated the return loss of bending radii. Many different kinds of crumpling (Fig. 32) may occur on a garment in this practical situation [72]. Fig. 33 illustrates the measured return loss of PIFA antenna matching capabilities under crumpling situations. There is a 40 MHz shift in resonant frequency higher, and a halving of the  $-10$  dB bandwidth, while the reflection coefficient of Case 2 reaches a maximum of roughly  $-5$  dB to indicate a reduction in performance. Using crumpling Case 3,

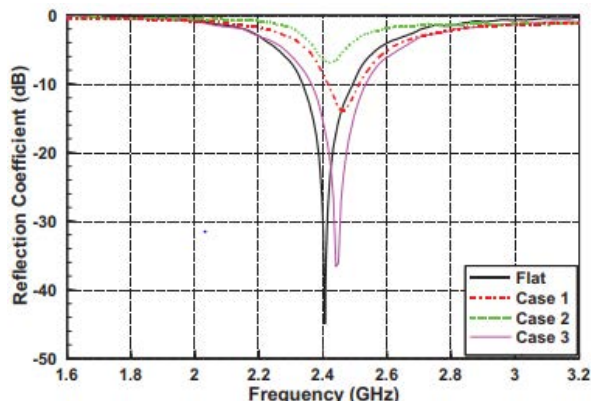


FIGURE 33. Measured crumpling antenna's return loss in various crumpling depths [72].

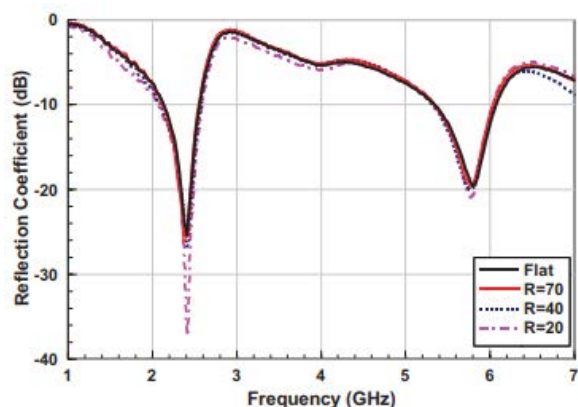


FIGURE 34. Measured  $S_{11}$  of bending dual-band antenna's H-plane [74].

the antenna is bent nearly 90 degrees, however the return loss of the antenna is only marginally affected, with the resonance frequency increasing by only 10 MHz. Bending and crumpling effect discussed in [64], this research work. As shown in Fig. 34, the  $S_{11}$  of the antenna was measured in H-plane bending (radii 20, 40 and 70 mm) states. As the bending radius decreases, the resonance frequency drops from 2200 MHz to 2050 MHz. In practical uses for clothe embedded with a textile antenna, it may be situated in many location, such as on the torso or a leg or arm. When the person change position, the clothing and, in particular the antennas are likely to be wrinkled, due to it being crushed joints. This Fig. 34 demonstrates the kind of folding depicted. Two crushed examples with standard 2D crumpling and bending patterns occur as a result of the arm being bent at the elbow. Fig. 35 depicts a plot of the measured return loss. In comparison to the antenna's flat-ground performance, both resonant bands had to endure some level of deterioration. When crumpled, the reflection coefficient decreases from  $-25$  dB for the flat antenna to  $-14$  dB for the worst crumpled example and the bandwidth decreases by 200 MHz. When the antenna is crumpled in the upper band by 5 mm, the resonant frequency changes by just 100 MHz, while the 10 mm crumple in the upper band yields

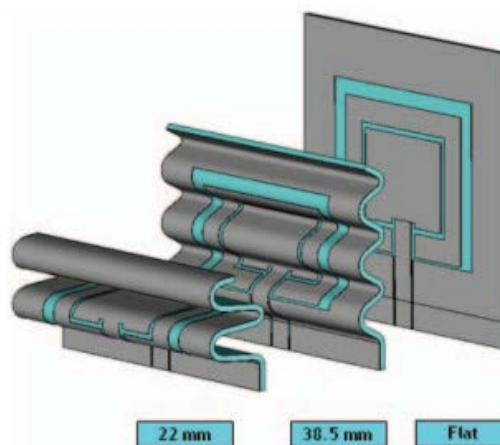


FIGURE 35. Prototype of flat and crumpling antenna [74].

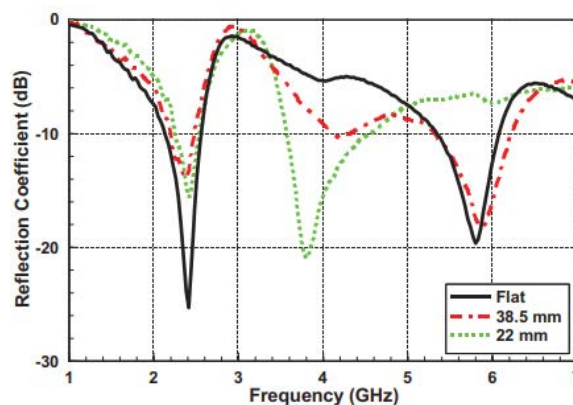


FIGURE 36. Measured return loss of crumpling antenna [74].

the best reflection coefficient at 3.8 GHz but at 5.8 GHz the reflection coefficient drops to  $-7$  dB. Even though the antenna's performance would be good enough for a lot of applications.

The majority of prior studies [73], on RFID tags have focused on their performance in a flat configuration. However, the effects of bending on antenna performance should be examined if a flexible substrate is employed, for example such as a wearable on-body system. Various different-sized cylinders ranging from 35 mm to 50 mm in radius were employed in order to accomplish it. Additionally, three primary radii were evaluated 30, 35, and 50 mm-diameter cylinders. As shown in Fig. 37, the RFID tag was created after 30 mm radius concave and convex bending. Such outcomes demonstrate that CPW monopoles situated above AMC sheet experience minor bending performance degradation. Fig. 40 shows an experiment [34], in which bend in both the vertical and horizontal directions was explored. The antenna's measurements are performed on polystyrene cylinders with 70, 80, 100, and 140 mm diameters. The varying diameters help test the frequency to see if it can be maintained while bent, as required for a wearable antenna

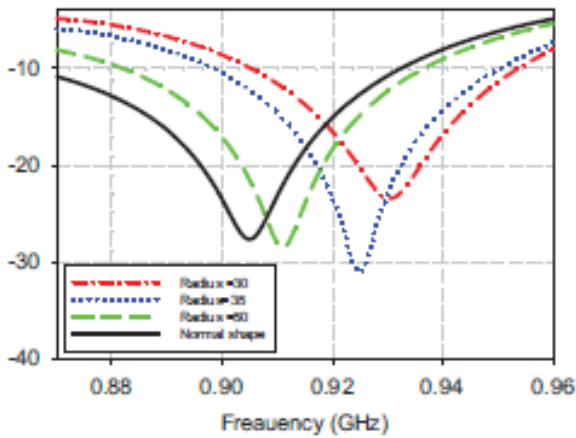


FIGURE 37. Antenna's bending and its  $S_{11}$  result [73].

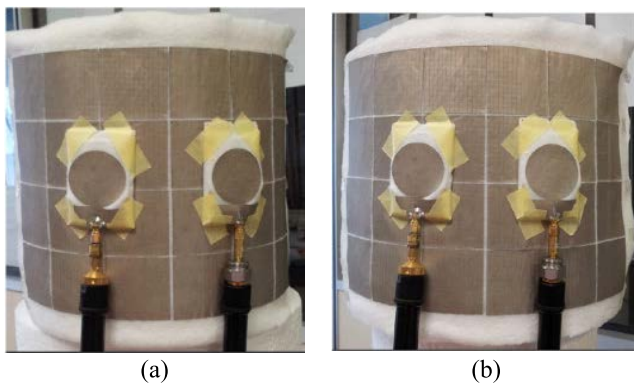


FIGURE 38. Textile CPW fabricated monopole antennas are combined with AMC sheet under bending conditions (a) large, (b) small [69].

that's both reliable and effective. Fig. 41 shows the return loss characteristics that were measured while the object was bent both vertically and horizontally. As the diameter is reduced, there is always a tiny upward tilt. For the horizontal instance, Fig. 41(b) indicates a 5 MHz shift to higher frequency at 50 mm which is insignificant. In general, the antenna functions within the target band without considerable frequency detuning, even when bent. The overall results obtained by the analysis detailed in Section III, as detailed in Table 2, were summarized.

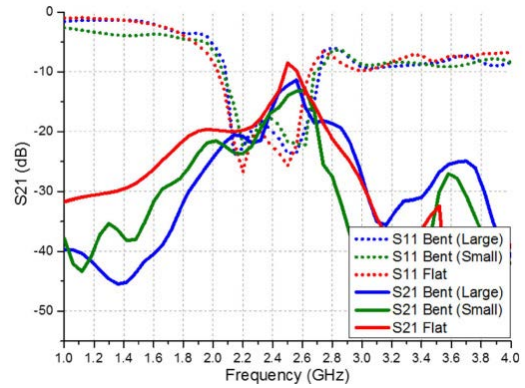


FIGURE 39. The textile CPW monopoles measured above the AMC under a bending situation were found to have an  $S_{11}$  and  $S_{21}$  value [69].

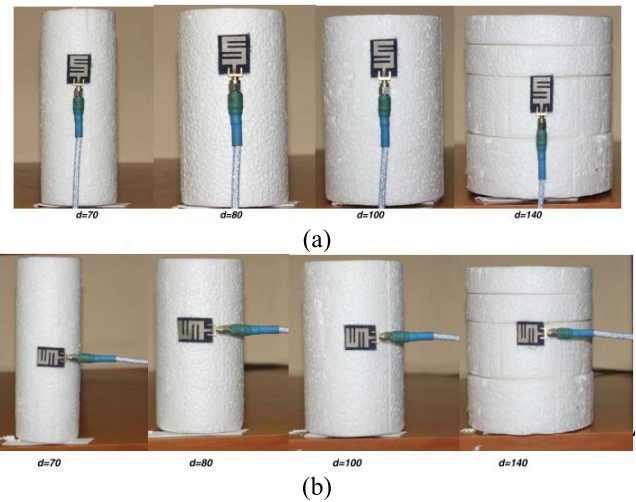


FIGURE 40. Pictures showing how the antenna is bent under various curvatures (a) y- axis and (b) x- axis [34].

Two cylinders made of polystyrene are used to study the bending of the human body using a set-up that mimics effect of the human body on the polystyrene. In this [60], proposed antenna and waveguide sheet testing with standard measured, the suggested antenna and waveguide sheet are tested with other wearable and body-centric measurements, such as bending and wetting studies. To simulate the dimensions of small and large torsos, polystyrene cylinders with 250 mm and 310 mm diameters, respectively, are employed in the measurement of bending resistance. Because the AMC sheet is very large, these cylinders that represent the size of a human torso are employed, and they are intended to be worn around the torso area. The small and large cylinders illustrate the CPW monopoles in Fig. 38 when AMC sheet is under bending condition. The CPW monopole S-parameters results depicted in Fig. 39 is obtain for the AMC sheet below bending and flat situations. For both small and big bending scenarios, as well as for the flat condition  $S_{11}$  and  $S_{21}$  graphs are shown. It is possible to establish a combination match between the bending and flat examples based on the S-parameter result.

**TABLE 2.** A summary of bending effects on the performances of wearable antennas.

Ref.	Substrate	Radius	Rad. efficiency (%)	BW (GHz)	Applications
[11]	Polyester fabric	Z, Y- axis	---	1.198–4.055	UWB
[30]	Jeans	---	---	3.09–3.94, 4.23–5.65	Wi-MAX, 5G lower band
[34]	Shieldit conducting fabric	35,40,50,70	79	2.4	ISM band
[36]	Polyester textile	0,10,20,30,40,50, 60,70,80,90,100	---	3.37	Wi-MAX
[39]	Denim	10 <sup>0</sup> ,60 <sup>0</sup> ,90 <sup>0</sup> ,150 <sup>0</sup>	96	7–28	WBAN, UWB
[48]	Thin planner textile	0 <sup>0</sup> ,45 <sup>0</sup> ,90 <sup>0</sup>	---	2.45	ISM band
[50]	Cotton	X,Y-bent condition, single crumple, severely crumple condition	---	2.45	ISM band
[51]	Felt	40,60,80	---	2.45	LTE, WLAN
[52]	Felt	X, Y- axis	---	2.45, 5.8	ISM band, WBAN
[54]	Polyester felt	0	---	2.4	ISM band
[55]	Polyester fabric	0	---	23–30, 24.5–28	5G
[56]	Demin fabric	0	---	2.45	ISM band
[59]	Polyester	x,y-bent condition	---	1.575	GPS application
[69]	Shieldit fabric	---	---	2.4	ISM band
[70]	Felt	39,45,55	---	2.45	ISM band
[71]	Zelt	15,25,35	74.04	2.35	ISM band
[72]	Zelt	Crumpling condition	---	2.43	ISM band
[74]	Felt	Bending (20,40,70) and Crumpling condition	---	2.45, 5.8	5.8 GHz and ISM band
[73]	Felt	30,35,50	---	0.915 GHz	UHF-RFID Tag
[53]	Woven cotton	Crumple condition	---	2.45	ISM band
[81]	Jeans	X,Y-bent condition	---	2.4	ISM band
[82]	Flexible felt	X,Y-bent and crumpling condition	57.5, 60.2	3.5, 5.8	Wi-MAX, ISM band
[83]	PI substrate	0 <sup>0</sup> , 10 <sup>0</sup> , 20 <sup>0</sup> , 35 <sup>0</sup>	---	5.8	ISM band

The S<sub>21</sub> peak for big bending cases at 2.56 GHz is –11.4 dB, and the small bending case at 2.62 GHz at a peak of –13.1 dB. The bent cases had a decrease in S<sub>21</sub> peaks of about –8.5 dB compared to the baseline case. Even though the S<sub>21</sub> peaks had shifted, a good transmission performance was still obtained, at the frequency of interest (2.45 GHz) for all cases. This meaning is to –13.3 dB, –13.5 dB, and –16 dB for flat, large bending and minor bending cases respectively.

In this section focuses a summary of bending effects on the performances of wearable antennas. Dielectric qualities and aspects of radiation around human skin are some of the other, issues with these antennas that need to be addressed with bending effect. Textile antennas are intended to be bent or conformed to a specific surface throughout the activity, and

hence diverse bending scenarios are needed to study changes in bending-dependent structure. More than nineteen research works that can be bent and attached to a person's body has been developed in this study, and polyester textile and denim has excellent performance on bending condition. Hence, all cases the resonant frequency shifted a bit compare to operating resonant frequency. Textiles and lightweight materials can be used for mechanical deformation, such as folding, because antennas worn by humans and other living creatures are common. Wearable antennas should be designed to be as symmetrical as feasible in order to minimize the impact on them when bent in a variety of directions. A system has been discovered in wearable important point to note is that AMC devices to be less prone to mechanical deformation. It has



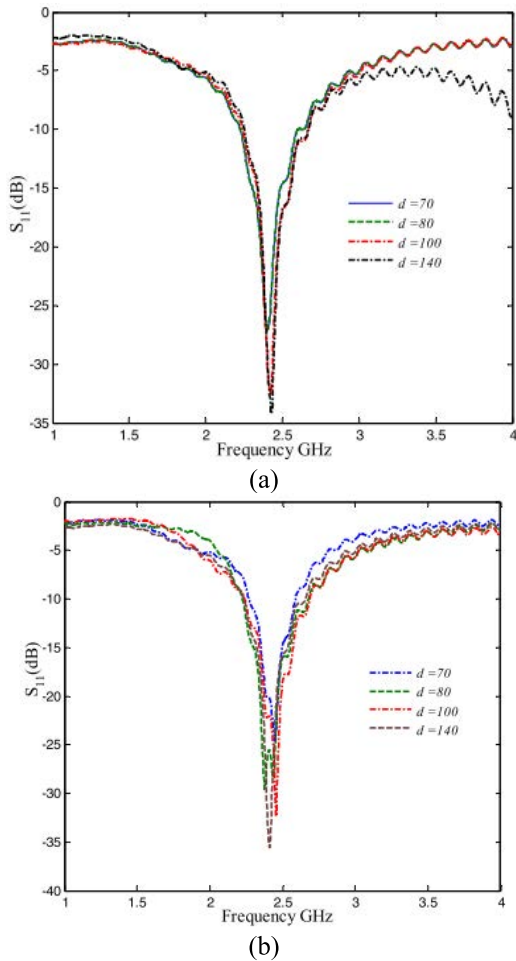


FIGURE 41. Measured of bending  $S_{11}$  (a) y-axis, (b) x-axis [34].

also been demonstrated that by utilizing the meta-surface, the effects of stretching as well as the presence of the human body in its vicinity can be reduced. The radiation effectiveness of CP antennas that are worn is also affected by bending. Rather, the resonant frequency of linearly polarized antennas is affected by bending because of differences in its effective range.

#### IV. SAR (SPECIFIC ABSORPTION RATE)

##### A. SAR VALUES

Along with making sure a wearable antenna is not too noticeable, designers must also think about the antenna's safety [11], [22], [36], [42], [48]. There are a variety of SAR values in Table 3 for various designs, with the maximum general exposure limiting to 1.6 W/kg (SAR 1 gm) or SAR being calculated as an average across a sample volume. The FCC and the ICNIRP/International Electrotechnical Commission (IEC) have set the limit at 2 W/kg (SAR 10 gm) [56]. The selection of phantoms and tissue models varies by group. Antenna and phantom separation factors influence the SAR results, as do various phantom sizes and tissue compositions [50], [52], [54]. When comparing the

patch antennas described in Table 3, which have the same size, operating frequency, and phantom arrangement, the patch antennas have equal SAR, but feeding via aperture coupling results in an enhanced SAR despite the antenna being twice as far away from the phantom. As a result, SAR values rely on factors such as the antenna type and shape in addition to the operating environment, making it impossible to draw general conclusions from a literature survey. Rather, such findings must be tailored to the application at hand. As can be seen, in Table 3 multiband antennas often have greater SAR values at higher frequency bands, whereas patch antennas operating at lower frequencies tend to have lower SAR values.

##### B. REDUCING SAR LEVELS

Several strategies have been developed to keep SAR levels as low as possible while maintaining higher efficiency. Because SAR of on-body antennas is dependent in part on near-field coupling to the body, the antenna with no ground plane (i.e. dipole) will have greater SAR values [23], [61], [75]–[77]. As a result, many of the strategies for reducing the SAR of off-body emitting antennas concentrate on changing the ground plane [78]. An example, of such a technique is the usage of EBG structures, also known as periodic conductive structures, which are used to filter electromagnetic waves within specific frequency bands [79]. Used the EBG to reflect radiation away from the body that the planar antenna would typically direct toward the body [76]. There were significant differences in SAR by using EBG structure geometry at 2.4 GHz, with showing the highest SAR at 0.0545 W/kg and without EBG shows 5.41 W/Kg [99], [100], [104], [106], [108]. Antennas can be made bulkier by adding additional ground plane components, and a truncated ground plane was created to prevent electric field hot spots [80]. Implementing an inverted ground section with a single-arm antenna meander near the feeding line minimizes the amount of interference around the feed while leaving the feed untouched [109]–[111]. For additional SAR reduction techniques, ferrite sheets and metamaterials can be integrated and Table 4 compares these methods.

This section discuss about SAR values and reduction methods of SAR. Radiating structures in wearable antennas applications have been the focus of this investigation. SAR is more closely examined in the context of wireless communications, where there are a plethora of radiating structures and research on exposure to the human body is of particular interest. A thorough anatomical structure is required for SAR analysis in implanted devices, since they are exposed directly to tissues. Different parts of the body are examined for their SAR levels. SAR computation approaches are well compared. The maximum SAR level was recorded 46.9 W/kg without applying technique and the minimum SAR value was 0.016 W/kg with applying technique (EBG). EBG, AMC and metamaterial technique shows batter effective performance to reduce the SAR level. Current approaches and estimating factors are evaluated for each scenario and discussed. The focus

TABLE 3. Comparison among different types of wearable antennas SAR values in W/Kg.

Source	Antenna design	Size (mm <sup>2</sup> )	Operational frequency (GHz)	SAR 1 gm (W/Kg)	SAR 10 gm (W/Kg)
[11]	Two triangle and parallel slots	70×50	1.198–4.055	---	0.0014
[22]	Folded ring shape antenna	60×60	2.45/3.45	0.2	0.1
[30]	C-shape etching slot	18×19	3.09–3.94, 4.23–5.65	---	0.353
[34]	Inverted E-shape antenna	30×20	2.4	---	---
[35]	Tuning fork shape antenna	25×25	3.4–4.3, 4.7–8.4, 10.3–14.1	Less than 1.6 W/kg	Less than 2 W/kg
[36]	E-shape patch antenna	50×50	3.37	---	---
[37]	---	42×13	2.45, 5.8	---	---
[38]	Cutting notch and slot patch antenna	25×25	2.96–11.6	---	1.6018
[41]	---	101×96	2.4	---	---
[42]	Rectangular patch antenna with PIN diodes	113×99	1.41–3	---	---
[43]	Ring shape patch antenna	40×40	3.01–5.30, 8.12–12.35	---	---
[44]	Planar inverted-F antenna	60×26	1.82–3.72	---	---
[45]	---	64.1×50	2.45	---	---
[48]	Dual port antenna	53.6×25.5	2.45	0.12	---
[49]	Rectangular patch antenna	90×90	2.45	---	---
[50]	Rectangular patch antenna with inset feed	51×45	2.45	---	0.486
[51]	Slotted split ring patch antenna	70×70	1.76–1.83, 2.36–2.76	---	0.01
[52]	Circular patch antenna	100×100	2.45, 5.8	0.042, 0.09	---
[53]	Reverse U & T shape slot patch antenna	58×63	2.45	---	---
[54]	T-shape slot inside rectangular patch	70×70	2.45	---	0.23
[55]	Dipole array antenna	251×2.7	23–30	---	---
[56]	Three slots and two stubs patch antenna	72×78	2.45	---	0.22
[75]	Ground coplanar wave guide antenna	60×50	7–28	0.25/0.7	0.071/0.171
[77]	Patch antenna with EBG ground plane	113×69.4	2.4	1.77	----
[84]	Patch antenna with PIFA	90×90	2.45	0.09	0.04
[85]	Rectangular patch	120×120	2.45	----	0.00544
[86]	Semi-circular metal patch with L slot AMC	66.8×66.8	2.45	----	0.15
[87]	3×3 FSS array	50.5×38	2.45	----	0.1641
[88]	2×2 EBG array	34×34	5.8	----	0.094
[89]	Pentagonal patch	70×85	0.9, 1.8	----	1.20, 1.81
[90]	AMC structure	20×30	5.8	Less than 1.6 W/Kg	Less than 2 W/Kg
[91]	Com-shape radiating patch	44×50	2.49	----	1.4
[92]	Metasurface antenna	50×50	5	0.291	0.0975
[93]	Slotted rectangular patch	70×60	2.45	0.087	0.043
[94]	2×2 circular array elements	46.722×52.722	2.5	0.2281	----
[95]	AMC backed	35×26	Tri-band	----	0.175
[96]	EBG structure	45.3×34.1	2.4/3.5/5.8	----	0.47/0.86/0.14

EBG (electromagnetic bandgap), AMC (artificial magnetic conductor)

**TABLE 4.** A summary of comparison in the performance of SAR reduction method.

Ref.	SAR reduction techniques	SAR without reduction (W/Kg)	SAR with Reduction Technique (W/Kg)	SAR per 1 or 10 gm tissue	Frequency (GHz)
[23]	EBG	7.18/7.96	0.31/0.42	10	2.45/5.8
[33]	Metal reflector	----	0.20	1	2.44
[61]	EBG	5.77/6.62	0.024/0.016	1	1.8/2.45
[76]	EBG	5.41	0.0545	1	2.4
[77]	EBG	2.36	1.77	10	2.4
[87]	FSS array	5.1972	0.1641	1	2.45
[90]	AMC	46.9	Less than 1.6	1	5.8
[97]	Metamaterial	7.78	0.0283	1	2.4
[98]	AMC	2	0.29	1	2.45
[99]	EBG	----	0.364/0.165	1/10	2.4
[100]	EBG	6.56	0.0251	1	2.4
[101]	AMC	4.2	1.24	10	2.4
[102]	Metasurface	6.6/11.7	0.0646/0.0268	1	5.2, 5.8
[103]	AMC	1.4	0.7	10	1.97
[104]	EBG	8.72	0.036	1	2.4
[105]	Flexible printed circuit board	----	0.474/0.11	1/10	5.8
[106]	EBG	2.814	0.956	1	2.54
[107]	Metamaterial	6.27	0.0671	10	UWB
[108]	EBG	7.23/4.18 7.23/2.06	0.972/0.668 2.80/1.51	1/10	2.45/5.8
[109]	AMC	----	0.903/0.338	1	3.5/5.8
[110]	Planar antenna	----	0.919/0.517	1	2.45/5.85
[111]	HIS	7.51/8.64	0.0257/0.0358	1	2.45

HIS (high impedance surface)

of this section is on the current SAR methods of reduction. SAR has a significant impact on a wide range of applications, and this survey article demonstrates this. Most of the case EBG, AMC structure is highly recommended for reducing SAR value.

## V. CONCLUSION

Wearable antennas are an essential component of wearable and portable equipment design. Because of their low weight, high adaptability, low cost, and conformal design, they are well suited for replacing outdated wireless networking and sensor technologies. There are a few areas in which wearable technology is thought to be of the most benefit. Aside from that, this article discusses the various materials and cutting-edge technology used to create these structures. Specification, operational frequency bands, smallest-dimensional precision, smooth fitting into wearing apparel, resilience to the rough environment, and the impact of bending scenarios, can all influence the type of material to use. Although

antennas require a low-loss dielectric material as well as highly conductive materials for effective receipt and transmission of electromagnetic radiation, extremely conductive products such as aluminum, metallic inks, conductive polymers, and PDMS integrated conductive fibers are modern varieties that are used as wearable antenna conductive components in a variety of applications. There were also other substrate materials that might be used because of their light weight and versatility. There can be no doubt that eliminating body coupling and implementing additional antenna capabilities are key parts of the specification. As a result, this feature was aimed at ensuring that the antenna function on the body would remain stable, as well as making it possible for antenna topologies to work with optimal performance. Finally, this article examined the performance of antennas design with substrate (textile material) and bendable antennas in a variety of radii, compared the results and SAR reduction technique. Consequently, antenna resonance frequency, SAR strength, and radiation pattern, are all affected by antenna bends.

## REFERENCES

- [1] S. N. Mahmood, A. J. Ishak, A. Ismail, A. C. Soh, Z. Zakaria, and S. Alani, "ON-OFF body ultra-wideband (UWB) antenna for wireless body area networks (WBAN): A review," *IEEE Access*, vol. 8, pp. 150844–150863, 2020.
- [2] A. Pellegrini, A. Brizzi, L. Zhang, K. Ali, Y. Hao, X. Wu, C. C. Constantinou, Y. Nechayev, P. S. Hall, N. Chahat, and M. Zhadobov, "Antennas and propagation for body-centric wireless communications at millimeter-wave frequencies: A review [wireless corner]," *IEEE Antennas Propag. Mag.*, vol. 55, no. 4, pp. 262–287, Aug. 2013.
- [3] S. Noor, N. Ramli, and N. L. Hanapi, "A review of the wearable textile-based antenna using different textile materials for wireless applications," *Open J. Sci. Technol.*, vol. 3, no. 3, p. 3, Oct. 2020.
- [4] D. B. Smith, D. Miniutti, T. A. Lamaheewa, and L. W. Hanlen, "Propagation models for body-area networks: A survey and new outlook," *IEEE Antennas Propag. Mag.*, vol. 55, no. 5, pp. 97–117, Oct. 2013.
- [5] H. Li, J. Du, X.-X. Yang, and S. S. C. Gao, "Low-profile all-textile multiband microstrip circular patch antenna for WBAN applications," *IEEE Antennas Wireless Propag. Lett.*, early access, Jan. 27, 2022, doi: 10.1109/LAWP.2022.3146435.
- [6] S. Yan, P. J. Soh, and G. A. E. Vandenbosch, "Wearable ultrawideband technology—A review of ultrawideband antennas, propagation channels, and applications in wireless body area networks," *IEEE Access*, vol. 6, pp. 42177–42185, 2018.
- [7] K. N. Paracha, S. K. A. Rahim, P. J. Soh, and M. Khalily, "Wearable antennas: A review of materials, structures, and innovative features for autonomous communication and sensing," *IEEE Access*, vol. 7, pp. 56694–56712, 2019.
- [8] A. Yadav, V. K. Singh, M. Chaudhary, and H. Mohan, "A review on wearable textile antenna," *J. Telecommun., Switching Syst. Netw.*, vol. 2, no. 3, pp. 37–41, 2015.
- [9] M. El Gharbi, R. Fernández-García, S. Ahyoud, and I. Gil, "A review of flexible wearable antenna sensors: Design, fabrication methods, and applications," *Materials*, vol. 13, no. 17, p. 3781, Aug. 2020.
- [10] M. Seyedi, B. Kibret, D. T. H. Lai, and M. Faulkner, "A survey on intrabody communications for body area network applications," *IEEE Trans. Biomed. Eng.*, vol. 60, no. 8, pp. 2067–2079, Aug. 2013.
- [11] X. Lin, Y. Chen, Z. Gong, B.-C. Seet, L. Huang, and Y. Lu, "Ultrawideband textile antenna for wearable microwave medical imaging applications," *IEEE Trans. Antennas Propag.*, vol. 68, no. 6, pp. 4238–4249, Jun. 2020.
- [12] C. Hertleer, H. Rogier, L. Vallozzi, and L. Van Langenhove, "A textile antenna for off-body communication integrated into protective clothing for firefighters," *IEEE Trans. Antennas Propag.*, vol. 57, no. 4, pp. 919–925, Apr. 2009.
- [13] S. Lakrit, S. Das, B. T. P. Madhav, and K. V. Babu, "An octagonal star shaped flexible UWB antenna with band-notched characteristics for WLAN applications," *J. Instrum.*, vol. 15, no. 2, Feb. 2020, Art. no. P02021.
- [14] P. Potey and K. Tuckley, "Design strategy of wearable textile antenna," in *Planar Antennas*. Boca Raton, FL, USA: CRC Press, 2021.
- [15] A. Akbarpour and S. Chamaani, "Ultrawideband circularly polarized antenna for near-field SAR imaging applications," *IEEE Trans. Antennas Propag.*, vol. 68, no. 6, pp. 4218–4228, Jun. 2020.
- [16] M. El Gharbi, M. Martínez-Estrada, R. Fernández-García, S. Ahyoud, and I. Gil, "A novel ultra-wide band wearable antenna under different bending conditions for electronic-textile applications," *J. Textile Inst.*, vol. 112, no. 3, pp. 437–443, Mar. 2021.
- [17] M. Klemm and G. Troester, "Textile UWB antennas for wireless body area networks," *IEEE Trans. Antennas Propag.*, vol. 54, no. 11, pp. 3192–3197, Nov. 2006.
- [18] R. P. Dwivedi and U. K. Kommuri, "Compact high gain UWB antenna using fractal geometry and UWB-AMC," *Microw. Opt. Technol. Lett.*, vol. 61, no. 3, pp. 787–793, Mar. 2019.
- [19] C. Sun, "A design of compact ultrawideband circularly polarized microstrip patch antenna," *IEEE Trans. Antennas Propag.*, vol. 67, no. 9, pp. 6170–6175, Sep. 2019.
- [20] C. Luo, I. Gil, and R. Fernández-García, "Wearable textile UHF-RFID sensors: A systematic review," *Materials*, vol. 13, no. 15, p. 3292, Jul. 2020.
- [21] L. Yang, "Review on wearable antenna design," in *Communications, Signal Processing, and Systems*. Singapore: Springer, 2021, pp. 731–742.
- [22] T. Le and T.-Y. Yun, "Wearable dual-band high-gain low-SAR antenna for off-body communication," *IEEE Antennas Wireless Propag. Lett.*, vol. 20, no. 7, pp. 1175–1179, Jul. 2021.
- [23] S. Zhu and R. Langley, "Dual-band wearable textile antenna on an EBG substrate," *IEEE Trans. Antennas Propag.*, vol. 57, no. 4, pp. 926–935, Apr. 2009.
- [24] V. Bhanumathi and S. Swathi, "Bandwidth enhanced microstrip patch antenna for UWB applications," *ICTACT J. Microelectron.*, vol. 4, no. 4, pp. 664–675, 2019.
- [25] Y. Yamada, "Dielectric properties of textile materials: Analytical approximations and experimental measurements—A review," *Textiles*, vol. 2, no. 1, pp. 50–80, Jan. 2022.
- [26] E. R. Radu, D. M. Panaitescu, L. Andrei, F. Ciuprina, C. A. Nicolae, A. R. Gabor, and R. Truşă, "Properties of polysiloxane/nanosilica nanodielectrics for wearable electronic devices," *Nanomaterials*, vol. 12, no. 1, p. 95, Dec. 2021.
- [27] C. Kissi, M. Särestöniemi, T. Kumpuniemi, M. Sonkki, S. Myllymäki, M. N. Scifri, and C. Pomalaza-Raez, "Directive low-band UWB antenna for in-body medical communications," *IEEE Access*, vol. 7, pp. 149026–149038, 2019.
- [28] S. Yan, P. J. Soh, and G. A. E. Vandenbosch, "Compact all-textile dual-band antenna loaded with metamaterial-inspired structure," *IEEE Antennas Wireless Propag. Lett.*, vol. 14, pp. 1486–1489, 2015.
- [29] A. Y. I. Ashyap, Z. Z. Abidin, S. H. Dahlan, H. A. Majid, S. M. Shah, M. R. Kamarudin, and A. Alomainy, "Compact and low-profile textile EBG-based antenna for wearable medical applications," *IEEE Antennas Wireless Propag. Lett.*, vol. 16, pp. 2550–2553, 2017.
- [30] M. M. H. Mahfuz, M. R. Islam, N. Sakib, M. H. Habaebi, R. Raad, and M. A. T. Sakib, "Design of wearable textile patch antenna using C-shape etching slot for wi-MAX and 5G lower band applications," in *Proc. 8th Int. Conf. Comput. Commun. Eng. (ICCCCE)*, Jun. 2021, pp. 168–172.
- [31] H. Shirakawa, E. J. Louis, A. G. MacDiarmid, C. K. Chiang, and A. J. Heeger, "Synthesis of electrically conducting organic polymers: Halogen derivatives of polyacetylene, (CH)<sub>x</sub>," *J. Chem. Soc., Chem. Commun.*, vol. 16, pp. 578–580, Jan. 1977.
- [32] K. Jayabharathy and T. Shanmuganatham, "Design of a compact textile wideband antenna for smart clothing," in *Proc. 2nd Int. Conf. Intell. Comput., Instrum. Control Technol. (ICICT)*, Jul. 2019, pp. 477–481.
- [33] A. G. Al-Sehemi, A. A. Al-Ghamdi, N. T. Dishovsky, N. T. Atanasov, and G. L. Atanasova, "Flexible and small wearable antenna for wireless body area network applications," *J. Electromagn. Waves Appl.*, vol. 31, nos. 11–12, pp. 1063–1082, Jun. 2017.
- [34] A. Y. I. Ashyap, Z. Z. Abidin, and S. H. Dahlan, "Inverted E-shaped wearable textile antenna for medical applications," *IEEE Access*, vol. 6, pp. 35214–35222, 2018.
- [35] A. Yadav, V. K. Singh, P. Yadav, A. K. Belya, A. K. Bhoi, and P. Barsocchi, "Design of circularly polarized triple-band wearable textile antenna with safe low SAR for human health," *Electronics*, vol. 9, no. 9, p. 1366, Aug. 2020.
- [36] S. B. Roshni, M. P. Jayakrishnan, P. Mohanan, and K. P. Surendran, "Design and fabrication of an E-shaped wearable textile antenna on PVB-coated hydrophobic polyester fabric," *Smart Mater. Struct.*, vol. 26, no. 10, Sep. 2017, Art. no. 105011.
- [37] S.-H. Li and J.-S. Li, "Smart patch wearable antenna on jeans textile for body wireless communication," in *Proc. 12th Int. Symp. Antennas, Propag. EM Theory (ISAPE)*, Dec. 2018, pp. 1–4.
- [38] A. Yadav, V. K. Singh, A. K. Bhoi, G. Marques, B. Garcia-Zapirain, and I. de la Torre Drez, "Wireless body area networks: UWB wearable textile antenna for telemedicine and mobile health systems," *Micromachines*, vol. 11, no. 6, p. 558, Jun. 2020.
- [39] S. N. Mahmood, A. J. Ishak, T. Saedi, A. C. Soh, A. Jalal, M. A. Imran, and Q. H. Abbasi, "Full ground ultra-wideband wearable textile antenna for breast cancer and wireless body area network applications," *Micromachines*, vol. 12, no. 3, p. 322, Mar. 2021.
- [40] K.-H. Wang and J.-S. Li, "Jeans textile antenna for smart wearable antenna," in *Proc. 12th Int. Symp. Antennas, Propag. EM Theory (ISAPE)*, Dec. 2018, pp. 1–3.
- [41] D. Ferreira, P. Pires, R. Rodrigues, and R. F. S. Caldeirinha, "Wearable textile antennas: Examining the effect of bending on their performance," *IEEE Antennas Propag. Mag.*, vol. 59, no. 3, pp. 54–59, Jun. 2017.
- [42] M. S. Shakhirul, M. Jusoh, A. H. Ismail, M. R. Kamarudin, H. A. Rahim, and T. Sabapathy, "Reconfigurable frequency with circular polarization for on-body wearable textile antenna," in *Proc. 10th Eur. Conf. Antennas Propag. (EuCAP)*, Apr. 2016, pp. 1–4.

- [43] V. K. Singh, S. Dhupkariya, and N. Bangari, "Wearable ultra wide dual band flexible textile antenna for WiMax/WLAN application," *Wireless Pers. Commun.*, vol. 95, no. 2, pp. 1075–1086, Jul. 2017.
- [44] Q. H. Dang, S. J. Chen, D. C. Ranasinghe, and C. Fumeaux, "A frequency-reconfigurable wearable textile antenna with one-octave tuning range," *IEEE Trans. Antennas Propag.*, vol. 69, no. 12, pp. 8080–8089, Dec. 2021.
- [45] A. Kavitha and J. N. Swaminathan, "Design of flexible textile antenna using FR4, jeans cotton and Teflon substrates," *Microsyst. Technol.*, vol. 25, no. 4, pp. 1311–1320, Apr. 2019.
- [46] W. G. Whittow, A. Chauraya, J. C. Vardaxoglou, Y. Li, R. Torah, K. Yang, S. Beeby, and J. Tudor, "Inkjet-printed microstrip patch antennas realized on textile for wearable applications," *IEEE Antennas Wireless Propag. Lett.*, vol. 13, pp. 71–74, 2014.
- [47] A. Chauraya, A. Chauraya, J. C. Vardaxoglou, Y. Li, R. Torah, K. Yang, S. Beeby, and J. Tudor, "Inkjet printed dipole antennas on textiles for wearable communications," *IET Microw., Antennas Propag.*, vol. 7, no. 9, pp. 760–767, Jun. 2013.
- [48] C. X. Mao, Y. Zhou, Y. Wu, H. Soewardiman, D. H. Werner, and J. S. Jur, "Low-profile strip-loaded textile antenna with enhanced bandwidth and isolation for full-duplex wearable applications," *IEEE Trans. Antennas Propag.*, vol. 68, no. 9, pp. 6527–6537, Sep. 2020.
- [49] B. Xu, R. J. Eike, A. Cliett, L. Ni, R. Cloud, and Y. Li, "Durability testing of electronic textile surface resistivity and textile antenna performance," *Textile Res. J.*, vol. 89, no. 18, pp. 3708–3721, Sep. 2019.
- [50] A. Anbalagan, E. F. Sundarsingh, V. S. Ramalingam, A. Samdaria, D. B. Gurion, and K. Balamurugan, "Realization and analysis of a novel low-profile embroidered textile antenna for real-time pulse monitoring," *IETE J. Res.*, pp. 1–8, Jul. 2020.
- [51] E. A. Mohammad, H. A. Rahim, P. J. Soh, M. F. Jamlos, M. Abdulmalek, and Y. S. Lee, "Dual-band circularly polarized textile antenna with splitting slot for off-body 4G LTE and WLAN applications," *Appl. Phys. A, Solids Surf.*, vol. 124, no. 8, p. 568, Jul. 2018.
- [52] L. Zhou, S. Fang, and X. Jia, "Dual-band and dual-polarised circular patch textile antenna for on-/off-body WBAN applications," *IET Microw., Antennas Propag.*, vol. 14, no. 7, pp. 643–648, Jun. 2020.
- [53] A. Anbalagan, E. F. Sundarsingh, and V. S. Ramalingam, "Design and experimental evaluation of a novel on-body textile antenna for unicast applications," *Microw. Opt. Technol. Lett.*, vol. 62, no. 2, pp. 789–799, Feb. 2020.
- [54] L. Yao, E. Li, J. Yan, Z. Shan, X. Ruan, Z. Shen, Y. Ren, and J. Yang, "Miniaturization and electromagnetic reliability of wearable textile antennas," *Electronics*, vol. 10, no. 9, p. 994, Apr. 2021.
- [55] E. Li, X. J. Li, B.-C. Seet, and X. Lin, "Ink-printed flexible wideband dipole array antenna for 5G applications," *Phys. Commun.*, vol. 43, Dec. 2020, Art. no. 101193.
- [56] P. M. Potey and K. Tuckley, "Design of wearable textile antenna for low back radiation," *J. Electromagn. Waves Appl.*, vol. 34, no. 2, pp. 235–245, Dec. 2019.
- [57] H. Kaur and P. Chawla, "Performance analysis of novel wearable textile antenna design for medical and wireless applications," *Wireless Pers. Commun.*, pp. 1–17, Jan. 2022.
- [58] M. Wagih, G. S. Hilton, A. S. Weddell, and S. Beeby, "2.4 GHz wearable textile antenna/rectenna for simultaneous information and power transfer," in *Proc. 15th Eur. Conf. Antennas Propag. (EuCAP)*, Mar. 2021, pp. 1–5.
- [59] N. I. Zaidi, M. T. Ali, N. H. A. Rahman, M. F. Yahya, and M. S. A. Nordin, "Analysis on different shape of textile antenna under bending condition for GPS application," *Bull. Electr. Eng. Inform.*, vol. 9, no. 5, pp. 1964–1970, Oct. 2020.
- [60] J. C. Wang, E. G. Lim, M. Leach, Z. Wang, and K. L. Man, "Review of wearable antennas for WBAN applications," *Int. J. Comput. Sci.*, vol. 43, no. 4, pp. 474–480, 2016.
- [61] S. Velan, E. F. Sundarsingh, M. Kanagasabai, A. K. Sarma, C. Raviteja, R. Sivasamy, and J. K. Pakkathillam, "Dual-band EBG integrated monopole antenna deploying fractal geometry for wearable applications," *IEEE Antennas Wireless Propag. Lett.*, vol. 14, pp. 249–252, 2014.
- [62] B. Tiwari, S. H. Gupta, and V. Balyan, "Design and analysis of wearable textile UWB antenna for WBAN communication systems," in *Proc. 2nd Int. Conf. Comput., Commun., Cyber-Secur.*, Singapore: Springer, 2021, pp. 141–150.
- [63] M. A. Kamatchi, V. Keralshalini, and A. Berlin, "Body Worn antenna for telemedicine applications," *Int. J. Emerg. Trends Sci. Technol.*, vol. 3, no. 2, pp. 9–12, 2017.
- [64] A. Lohia, J. Pal, N. Kushwaha, and S. Shreevas, "Racket shape textile antenna for triple-band frequency applications," *Emerg. Mater. Adv. Des. Wearable Antennas*, pp. 165–179, 2021.
- [65] A. Yadav, V. K. Singh, and H. Mohan, "Design of a U-shaped circularly polarized wearable antenna with DGS on a fabric substrate for WLAN and C-band applications," *J. Comput. Electron.*, vol. 18, no. 3, pp. 1103–1109, Sep. 2019.
- [66] A. K. Jain, B. K. Kanaujia, S. Dwari, G. P. Pandey, and D. K. Singh, "Wideband circularly polarized magnetoelectric dipole antenna with I-slot for C-band applications," *J. Comput. Electron.*, vol. 18, no. 2, pp. 660–670, Jun. 2019.
- [67] A. S. M. Sayem, R. B. V. B. Simorangkir, K. P. Esselle, A. Lalbakhsh, D. R. Gawade, B. O'Flynn, and J. L. Buckley, "Flexible and transparent circularly polarized patch antenna for reliable unobtrusive wearable wireless communications," *Sensors*, vol. 22, no. 3, p. 1276, Feb. 2022.
- [68] L. Song and Y. Rahmat-Samii, "A systematic investigation of rectangular patch antenna bending effects for wearable applications," *IEEE Trans. Antennas Propag.*, vol. 66, no. 5, pp. 2219–2228, May 2018.
- [69] K. Kamardin, M. K. A. Rahim, P. S. Hall, N. A. Samsuri, T. A. Latef, and M. H. Ullah, "Textile artificial magnetic conductor jacket for transmission enhancement between antennas under bending and wetness measurements," *Appl. Phys. A, Solids Surf.*, vol. 122, no. 4, p. 423, Mar. 2016.
- [70] B. Hu, G.-P. Gao, L.-L. He, X.-D. Cong, and J.-N. Zhao, "Bending and on-arm effects on a wearable antenna for 2.45 GHz body area network," *IEEE Antennas Wireless Propag. Lett.*, vol. 15, pp. 378–381, 2016.
- [71] U. Ali, S. Ullah, M. Shafi, S. A. A. Shah, I. A. Shah, and J. A. Flint, "Design and comparative analysis of conventional and metamaterial-based textile antennas for wearable applications," *Int. J. Numer. Model., Electron. Netw., Devices Fields*, vol. 32, no. 6, Nov. 2019, Art. no. e2567.
- [72] Q. Bai and R. Langley, "Textile PIFA antenna bending," in *Proc. Loughborough Antennas Propag. Conf.*, Nov. 2011, pp. 1–4.
- [73] M. E. Bakkali, M. Martinez-Estrada, R. Fernandez-Garcia, I. Gil, and O. E. Mrabet, "Effect of bending on a textile UHF-RFID tag antenna," in *Proc. 14th Eur. Conf. Antennas Propag. (EuCAP)*, Mar. 2020, pp. 1–5.
- [74] Q. Bai and R. Langley, "Wearable EBG antenna bending and crumpling," in *Proc. Loughborough Antennas Propag. Conf.*, Nov. 2009, pp. 201–204.
- [75] S. N. Mahmood, A. J. Ishak, T. Saedi, A. C. Soh, A. Jalal, M. A. Imran, and Q. H. Abbasi, "Full ground ultra-wideband wearable textile antenna for breast cancer and wireless body area network applications," *Micro-machines*, vol. 12, no. 3, p. 322, Mar. 2021.
- [76] A. Y. I. Ashyap, Z. Zainal Abidin, S. H. Dahlan, H. A. Majid, M. R. Kamarudin, A. Alomaiy, R. A. Abd-Alhameed, J. S. Kosha, and J. M. Noras, "Highly efficient wearable CPW antenna enabled by EBG-FSS structure for medical body area network applications," *IEEE Access*, vol. 6, pp. 77529–77541, 2018.
- [77] U. Ali, S. Ullah, J. Khan, M. Shafi, B. Kamal, A. Basir, J. A. Flint, and R. D. Seager, "Design and SAR analysis of wearable antenna on various parts of human body, using conventional and artificial ground planes," *J. Electr. Eng. Technol.*, vol. 12, no. 1, pp. 317–328, Jan. 2017.
- [78] K. N. Paracha, S. K. A. Rahim, P. J. Soh, M. R. Kamarudin, K. G. Tan, Y. C. Lo, and M. T. Islam, "A low profile, dual-band, dual polarized antenna for indoor/outdoor wearable application," *IEEE Access*, vol. 7, pp. 33277–33288, 2019.
- [79] J. O. Abolade, D. B. O. Konditi, and V. M. Dharmadhikary, "Compact bio-inspired dual-band uniplanar electromagnetic bandgap-backed antenna for wearable applications," *Int. J. RF Microw. Comput.-Aided Eng.*, vol. 31, no. 12, Dec. 2021, Art. no. e22880.
- [80] S. Bhattacharjee, M. Mitra, and S. R. B. Chaudhuri, "An effective SAR reduction technique of a compact meander line antenna for wearable applications," *Prog. Electromagn. Res. M*, vol. 55, pp. 143–152, 2017.
- [81] S. Mallavarapu and A. Lokam, "Circuit modeling and analysis of wearable antennas on the effect of bending for various feeds," *Eng., Technol. Appl. Sci. Res.*, vol. 12, no. 1, pp. 8180–8187, Feb. 2022.
- [82] H. Yang, X. Liu, Y. Fan, and L. Xiong, "Dual-band textile antenna with dual circular polarizations using polarization rotation AMC for off-body communications," *IEEE Trans. Antennas Propag.*, early access, Jan. 5, 2022, doi: 10.1109/TAP.2021.3138504.
- [83] J. Zhang, J. Huang, P. Sun, F. Meng, J. Zhang, and P. Zhao, "Analysis method of bending effect on transmission characteristics of ultra-low-profile rectangular microstrip antenna," *Sensors*, vol. 22, no. 2, p. 602, Jan. 2022.
- [84] I. Gil and R. Fernandez-Garcia, "SAR impact evaluation on jeans wearable antennas," in *Proc. 11th Eur. Conf. Antennas Propag. (EuCAP)*, Mar. 2017, pp. 2187–2190.

- [85] E. S. Florence, M. Kanagasabai, and G. N. M. Alsath, "An investigation of a wearable antenna using human body modelling," *Appl. Comput. Electromagn. Soc. J.*, vol. 29, no. 10, pp. 777–783, Oct. 2014.
- [86] B. Yin, J. Gu, X. Feng, B. Wang, Y. Yu, and W. Ruan, "A low SAR value wearable antenna for wireless body area network based on AMC structure," *Prog. Electromagn. Res. C*, vol. 95, pp. 119–129, 2019.
- [87] B. Sugumaran, R. Balasubramanian, and S. K. Palaniswamy, "Reduced specific absorption rate compact flexible monopole antenna system for smart wearable wireless communications," *Eng. Sci. Technol.*, vol. 24, no. 3, pp. 682–693, Jun. 2021.
- [88] V. R. Keshwani and S. S. Rathod, "Assessment of SAR reduction in wearable textile antenna," in *Proc. Int. Conf. Commun. Inf. Comput. Technol. (ICCICT)*, Jun. 2021, pp. 1–5.
- [89] P. Shirvani, F. Khajeh-Khalili, and M. H. Neshati, "Design investigation of a dual-band wearable antenna for tele-monitoring applications," *AEU Int. J. Electron. Commun.*, vol. 138, Aug. 2021, Art. no. 153840.
- [90] P. Saha, D. Mitra, and S. K. Parui, "Control of gain and SAR for wearable antenna using AMC structure," *Radioengineering*, vol. 30, no. 1, pp. 81–88, Apr. 2021.
- [91] D. Gopi, P. V. Kokilagadda, S. Gupta, and V. R. K. R. Dodda, "Asymmetric coplanar strip-fed textile-based wearable antenna for MBAN and ISM band applications," *Int. J. Numer. Model., Electron. Netw., Devices Fields*, vol. 34, no. 6, Nov. 2021.
- [92] G. Gao, H. Meng, W. Geng, B. Zhang, Z. Dou, and B. Hu, "Design of a wide bandwidth and high gain wearable antenna based on nonuniform metasurface," *Microw. Opt. Technol. Lett.*, vol. 63, no. 10, pp. 2606–2613, Oct. 2021.
- [93] A. Shah and P. Patel, "E-textile slot antenna with spurious mode suppression and low SAR for medical wearable applications," *J. Electromagn. Waves Appl.*, vol. 35, no. 16, pp. 2224–2238, Nov. 2021.
- [94] N. Ramanpreet, M. Rattan, and S. S. Gill, "Compact and low profile planar antenna with novel metastructure for wearable MBAN devices," *Wireless Pers. Commun.*, vol. 118, no. 4, pp. 3335–3347, Jun. 2021.
- [95] B. T. P. Madhav, J. Vani, R. R. Priyanka, B. P. Nadh, and M. C. Rao, "Concentric ring loaded monopole antenna with AMC backed for Wearable applications," *J. Phys., Conf. Ser.*, vol. 1804, no. 1, Feb. 2021, Art. no. 012191.
- [96] W. El May, I. Sfar, J. M. Ribero, and L. Osman, "Design of low-profile and safe low SAR tri-band TEXTILE EBG-based antenna for IoT applications," *Prog. Electromagn. Res. Lett.*, vol. 98, pp. 85–94, 2021.
- [97] A. Y. I. Ashyap, Z. Zainal Abidin, S. H. Dahlan, H. A. Majid, and G. Saleh, "Metamaterial inspired fabric antenna for wearable applications," *Int. J. RF Microw. Comput. Aided Eng.*, vol. 29, no. 3, Mar. 2019, Art. no. e21640.
- [98] S. M. Saeed, C. A. Balanis, C. R. Birtcher, A. C. Durgun, and H. N. Shaman, "Wearable flexible reconfigurable antenna integrated with artificial magnetic conductor," *IEEE Antennas Wireless Propag. Lett.*, vol. 16, pp. 2396–2399, 2017.
- [99] A. Y. I. Ashyap, Z. Z. Abidin, S. H. Dahlan, H. A. Majid, and F. C. Seman, "A compact wearable antenna using EBG for smart-watch applications," in *Proc. Asia-Pacific Microw. Conf. (APMC)*, Nov. 2018, pp. 1477–1479.
- [100] A. Y. I. Ashap, Z. Z. Abidin, S. H. Dahlan, H. A. Majid, S. K. Yee, G. Saleh, and N. A. Malek, "Flexible wearable antenna on electromagnetic band gap using PDMS substrate," *TELKOMNIKA (Telecommun. Comput. Electron. Control)*, vol. 15, no. 3, p. 1454, Sep. 2017.
- [101] K. Agarwal, Y.-X. Guo, B. Salam, and L. C. W. Albert, "Latex based near-endfire wearable antenna backed by AMC surface," in *IEEE MTT-S Int. Microw. Symp. Dig.*, Dec. 2013, pp. 1–3.
- [102] H.-L. Yang, W. Yao, Y. Yi, X. Huang, S. Wu, and B. Xiao, "A dual-band low-profile metasurface-enabled wearable antenna for WLAN devices," *Prog. Electromagn. Res. C*, vol. 61, pp. 115–125, 2016.
- [103] S. I. Kwak, D. Sim, J. H. Kwon, and Y. J. Yoon, "Design of PIFA with metamaterials for body-SAR reduction in wearable applications," *IEEE Trans. Electromagn. Compat.*, vol. 59, no. 1, pp. 297–300, Feb. 2017.
- [104] A. Y. I. Ashyap, Z. Z. Abidin, S. H. Dahlan, H. A. Majid, M. R. Kamarudin, and R. A. Abd-Alhameed, "Robust low-profile electromagnetic band-gap-based on textile wearable antennas for medical application," in *Proc. Int. Workshop Antenna Technol., Small Antennas, Innov. Struct., Appl. (iWAT)*, 2017, pp. 158–161.
- [105] J. H. Kim and H. M. Lee, "Low specific absorption rate wearable antenna for WLAN band applications," in *Proc. 4th Eur. Conf. Antennas Propag.*, Apr. 2010, pp. 1–5.
- [106] M. I. Ahmed, E. A. Abdallah, and H. M. Elhennawy, "SAR investigation of novel wearable Reduced-coupling microstrip antenna array," *Int. J. Eng.*, vol. 15, no. 3, pp. 78–86, 2015.
- [107] H. Yalduz, T. E. Tabaru, V. T. Kilic, and M. Turkmen, "Design and analysis of low profile and low SAR full-textile UWB wearable antenna with metamaterial for WBAN applications," *AEU Int. J. Electron. Commun.*, vol. 126, Nov. 2020, Art. no. 153465.
- [108] G. Gao, B. Hu, S. Wang, and C. Yang, "Wearable planar inverted-F antenna with stable characteristic and low specific absorption rate," *Microw. Opt. Technol. Lett.*, vol. 60, no. 4, pp. 876–882, Apr. 2018.
- [109] M. El Atrash, M. A. Abdalla, and H. M. Elhennawy, "A wearable dual-band low profile high gain low SAR antenna AMC-backed for WBAN applications," *IEEE Trans. Antennas Propag.*, vol. 67, no. 10, pp. 6378–6388, Oct. 2019.
- [110] T. T. Le and T.-Y. Yun, "Miniaturization of a dual-band wearable antenna for WBAN applications," *IEEE Antennas Wireless Propag. Lett.*, vol. 19, no. 8, pp. 1452–1456, Aug. 2020.
- [111] A. Y. I. Ashyap, S. F. B. Dahlan, Z. Z. Abidin, S. K. A. Rahim, H. A. Majid, A. S. Alqadami, and M. El Atrash, "Fully fabric high impedance surface-enabled antenna for wearable medical applications," *IEEE Access*, vol. 9, pp. 6948–6960, 2021.

...